LIQUID PHASE VELOCITY OF TURBULENT DISPERSED BUBBLES FLOW IN LARGE DIAMETER HORIZONTAL PIPES

by

Aouni A. LAKIS and Nguyen D. TRINH

Technical Report

No. EPM/RT 88-24

1988

Department of Mechanical Engineering

Ecole Polytechnique de Montreal

University of Montreal

P.O. Box 6079, Station A, Montreal

Quebec, Canada, H3C 3A7

TABLE OF CONTENTS

LIQUID PHASE VELOCITY OF TURBULENT DISPERSED BUBBLES FLOW IN LARGE DIAMETER HORIZONTAL PIPES

ABSTRACT

Measurement methods of impact pressure in two-phase bubble flow are discussed leading to the design of a liquid phase isolator. This simple device, with a miniature pressure transducer makes it possibles to measure the impact pressure of the liquid phase in gas-liquid mixture flow from which , the liquid velocity can then be deduce knowing the local void fraction.

Using a measured void fraction, pressure drop, mixture and phase velocities and liquid phase distribution can be predicted by either finding new correlations or by a developed numerical model.

Experiments were performed in 8-in. diameter horizontal pipes with a 0.30 maximum flow volumetric quality. It was found that in high turbulence ($R_* = 2 \times 10^6$), the liquid velocity profile behaves like that of single liquid flow, the symmetry of the profile being changed when flow volumetric quality varies from about 12% to its maximum value.

The uniformity of radial pressure distribution in fully developed dispersed bubbles flow is due to that of the void fraction, which in turn strongly influences the radial phase distribution. Liquid velocity distribution was found to be uniform in the radial plane. In the transversal plane owing to a large concentration of bubbles in the upper part of the pipe and their velocities being generally lower than those of the liquid phase in the actual case, the liquid velocity decreased because the drag effect of local displaced bubbles. Liquid velocity was distributed non-uniformly in the transversal plane.

The effects of gravity (assuming it is stabilized in steady fully developed flow), interfacial forces and the turbulence structure of the continuous phase seem to have a great influence on the liquid phase velocity distribution in a large horizontal pipe.

REMERCIEMENTS

Ce document a pu être publié grâce à une subvention du Conseil de recherches en sciences et en génie du Canada (CRSNG) (Subv: no. A-8814) et le F.C.A.R. du Québec (Subv: no. CRP-2060).

Nous tenons à remercier Mme Danielle Therrien qui a dactylographié tous nos textes, modèles et formulaire.

Dépôt légal, 2e trimestre 1986
Bibliothèque nationale du Québec
Bibliothèque nationale du Canada

Pour se procurer une copie de ce document, s'adresser aux:

Editions de l'Ecole Polytechnique de Montréal
Ecole Polytechnique de Montréal
Case postale 6079, Succursale A
Montréal (Québec) H3C 3A7
(514) 340-4000

Compter 0,10$ par page (arrondir au dollar le plus près) et ajouter 3,00$ (Canada) pour la couverture, les frais de poste et la manutention. Régler en dollars canadiens par chèque ou mandat-poste au nom de l'Ecole Polytechnique de Montréal. Nous n'honorerons que les commandes accompagnées d'un paiement, sauf s'il y a eu entente préalable dans le cas d'établissements d'enseignement, de sociétés ou d'organismes canadiens.

NOMENCLATURE

D	Nominal diameter of the pipe.
P_M	Static pressure of mixture flow.
Q_{Lo}	Initial volumetric flow rate of liquid.
X_o	Flow volumetric quality ($Q_{Lo}/ Q_{go} + Q_{Lo}$).
U^*	Friction velocity.
U^*_{2P}	Friction velocity of two-phase flow.
U_{L1P}	Single phase liquid velocity (water flow).
U_{L2P}	Liquid phase velocity of an air-liquid flow.
U_o	Superficial or initial phase velocity.
U_{Lo}	Superficial or initial liquid velocity.
U_M	Velocity of mixture flow.
$\bar{U}$	Average velocity.
Y	Transversal direction.
Z	Longitudinal direction.
α	Local void fraction.
ε	Eddy diffusivity.
ρ	Density of fluid.
ν	Kinematic viscosity of fluid.
μ	Absolute or dynamic viscosity of fluid.
ΔP	Differential pressure of liquid phase in a mixture flow.
τ_{Lo}	Turbulent shear stress of two-phase flow = τ_{int}
τ_w	Wall shear stress.

τ_{wzF} Wall shear stress of two-phase flow.

ϕ Non-dimensional velocity of liquid.

LIST OF FIGURES

CHAPTER 1

INTRODUCTION

Liquid velocity plays an important role in physical modeling of both single and two-phase flows. If a liquid is the continuous phase of a mixture flow, knowledge of its velocity distribution permits a better understanding the turbulence structure of the flow and the phase distribution mechanism.

The linear velocity of liquid in a gas-liquid mixture flow may be determined in the same way as that in a liquid single phase flow. Methods currently used include the injection into the flow of a solution and the measurement the of transit time of fluid particles between two successive electrodes (Sodium chloride, Jepsen and Ralph [1]; salt water or hot water, Kobayashi Andirino [2], Serizawa et al. [3]), or measurement of the oxygen reduction velocity appearing at the surface of the electrodes. this velocity varies with that of the flow (electrochemical method, Mitchell and Hanratty [4] electrodiffusion, Kozmienko et al. [5], the power law of 1/6 to 1/7 being found in the turbulent case which indicates that the profiles are very close to those noted in turbulent single phase flow. In equalizing the static pressure just at the entrance of the probe and at the same axial position in the flow (isokinetic sampling method), Alia et al. [6], Jepsen and Ralph [1] the

liquid velocity of a vertical dispersed annular flow may be deduced from the data of pressure, mass flow rate and void fraction. Using the signal analysis method proposed by Delhave [7], Serizawa et al. [8], [(] and Galaup [10] have obtained the liquid velocity with a hot film anemometer and the amplitude histogram of a multichannel analyzer. The power law of 1/7 for liquid velocity distribution was also reported in Ohba et al, [11] with a laser Doppler velocimeter in a vertical upward/downward bubble flow. Brown et al. [12] suppose that the liquid velocity profile can be represented by a parabolic function in which a correction factor varying from 0 to 1 is added. The numerical model of Sato and Sekoquchi, [13] verifies experimental work carried out in a vertical rectangular tube of 25 x 50 mm, where the shear stress of the liquid phase (air-water flow) is separated into two parts: one related to the inherent turbulence of the liquid independent of the existence of the bubble, the other to the supplementary turbulence of the liquid by bubble agitation. Bankott [14] proposes a power law of distribution for each velocity and void fraction profile, where the shear stress is presumed to be uniform over all sections of the pipe. Brown and Kranich [15], on the other hand propose a logarithmic distribution for the velocity of an air-water bubble flow. Krashcheev and Muranov [16] calculate the velocity of an annular dispersed water vapour flow by replacing the flow by a homogeneous medium, shear stress and the core film interface velocity are of the same order of

magnitude. Application of Prandtl's mixing length theory in the analytical treatment of velocity distribution is also adopted by Bankoft [14], Levy [17] and Gorin [18].

The general consensus is that most investigations have dealt with local liquid phase distribution and mixture velocity which is reliable for two-phase flow in small diameter pipe.

In this investigation, we first develop a measuring technique for the liquid phase velocity of a dispersed bubble flow in large diameter horizontal pipes. Secondly, the relationship between the phase distribution mechanism and the turbulence structure in the continuous phase will be expressed initially in terms of linear liquid velocities (in single phase and two-phase flows) and the measured void fraction. Finally, velocity distributions between experimental data and those predicted numerically will be compared, where the numerical work was developed based on the model of Sato and Sekoguchi [13] which has been proposed for bubble flow.

CHAPTER 2

EXPERIMENT DESCRIPTION

The horizontal air-water flow facility is shown schematically in Figure 1. This facility has been installed and used by Lakis [19] for studying wall pressure fluctuations in an annularly dispersed bubbly flow.

Briefly, water flows from a 15000 USG open reservoir tank through the loop at a rate of 2000 to 5000 USGPM and mixes with compressed air to produce a two-phase flow. Experiments were conducted in a series of horizontal pipes of 8-in. nominal diameter and 1360 ft total distance from the mixer. Pipelines consist of interchangeable PVP pipes, a steel pipe (for installing the wall pressure transducers), and a plexiglass pipe. The evolution of the flow can be visually monitored by moving the clear section along the pipe.

The piezometric lines were picked up using several pressure taps located along and around the pipes. Pressure drop was measured with Bourdon or pressure transducers which were used to evaluate the friction velocity in two-phase flow.

The maximum flow volumetric quality (ratio of gas volumetric flow rate to total volumetric flow rate) is 30% due to the loop

capacity. This results in the following three observable flow regimes: slug flow, dispersed slug waved flow and stratified dispersed bubbles flow as shown in Figure 2.

Experimental conditions summarized in Table 1 clearly refer to the case of stratified dispersed bubbles flow.

Experimental and numerical analyses are carried out fully developed flow conditions. preliminary examination of some flow parameters and visual observation at the clear section suggests that the flow is supposed to be completely developed at 130 D from the mixer, where D is the nominal diameter of the pipe. More detail on experimental apparatus and procedure may be found in Trinh [20].

CHAPTER 3

PRINCIPLE OF MEASUREMENT OF LOCAL LIQUID PHASE VELOCITY

3.1 Use of Pitot tube and pressure transducers

Application of Pitot tube and differential pressure transducers in two-phase flow has been adopted by several investigators, notably Halbronn [21], Gill et al. [22] for studying annularly dispersed flow; Kinoshita et Murasaki [2] for analysing pulsating phenomena; Zigami et al. [23] for measuring liquid phase variables; Fincke and Deason [24], Lakis and Mohamed [25] for experimenting with dispersed bubbles flow, etc.

In general, the interpretation of measured impact pressure is some difficult unless the measured variable is well sepcified. the isokinetic sampling method was then adopted by Anderson and Manzouranis [26] in studying the flow with air predominating; Jepsen and Ralph [1], Shires and Riley [27], Alia et al. [6] in obtaining information about one phase in an annularly dispersed flow.

The use of the Pitot tube in two-phase flow is efficient when its opening diameter is smaller to a reasonable extent than that of the elements in the dispersed phase. the presence of bubbles in the Pitot tube itself or in the connection tubes

forms empty spaces, the next bubbles tending to accumulate there before yielding their own energy to the static fluid filling the tube. The accumulation of bubbles increases over time and caused misinterpretation of the output readings. However, a small opening dimension of the Pitot tube results in a very long measuring time. The currently adopted method is the use of current of water under pressure with a set of three nozzle taps in which flow remains constant in the direction of the manometer tap. Another approach suitable for this study is an air current constantly flowing in the direction of the manometer pressure taps at a given pressure. The current must be adjusted automatically in such a what as to maintain equilibrium with the pressure exercised during the experiment. The difference between initial and final values represents the desired total pressure.

In this investigation, the average impact pressure of a two-phase flow is initially determined by means of a Pitot tube with a diaphragmatic differential pressure transducer. Air is purged in two clear cylindrical containers, which are always filled with water before entering both sides of the pressure transducer. Air bubbles can later be freely evacuated to the atmosphere by means of a valve situated on the top of each container or air-purger. the diagram of measurement is illustrated in Figure 3.

Unfortunately, this method is unsuccessful in actual flows due to the presence of bubbles in the measurement system after some measuring periods as the photographs in Figure a shown. Also, the use water current under pressure could not guarantee the absence of bubbles in the Pitot tube itself at the over actual range of flow volumetric quality.

3.2 Isolation of liquid in two-phase gas-liquid flow

Assuming that the pressure signals obtained at stagnation point result uniquely from the liquid phase, the deduced velocity will be that of the liquid phase in the mixture. In order words, it involves minimizing of neutralizing the kinetic energy of the gas phase at this point without disturbing the dynamic behaviour of the liquid phase.

A so-called liquid isolator has been designed for this purpose. Using such an isolator mounted on a miniature differential pressure transducer, air bubbles are eliminated when passing the stagnation point. The rectilinear opening of the isolator is in contact simultaneously with the pressure-sensitive area of the transducer and surrounding fluid.

In single phase water flow, this contact makes it possible to state that the measured pressure is the same type as that obtained by the transducer alone, although its magnitude would

be corrected by a calibration procedure.

In two-phase flow, it the form and dimension of the isolator are designed in such a way as to eliminate to the maximum the impact of bubbles in front of the sensor with a minimum fluctuation around this point, it may be concluded that the major part of the kinetic energy received come from the liquid phase. Liquid velocity would be calculated from the known local density of the liquid phase and the calibration procedure of isolator in single water flow.

According to visual observations of pressure signals traced on a memorized oscilloscope, the conical form with a rectilinear opening width of 0.020 in. offers minimum fluctuation even at maximum flow to volumetric quality (30%).

The dimensions of the pressure transducer and its suppport are given in Figure 5. The optimum design of the liquid isolator and the measurement device for liquid phase impact pressure are given in Figures 6.a and 6.b, respectively.

Examples of recorded pressure signals and their broadband frequency spectrum obtained by the isolator an transducer system in single and two-phase flows are shown in Figure 7.a and 7.b, respectively.

3.3 Equipment and calibration

The principle of the average dynamic pressure measurement of a mixture and liquid phase is illustrated schematically in Figure 8.

Calibration of the liquid isolator is carried out in single water flow for various water flow rates. The transducer is first placed at the pipe axis and at each given flow rate the impact pressure is noted at the output of an integrating digital voltmeter. The same procedure is repeated with the transducer and liquid isolator system. A comparison resulting measured pressures may be made in the graph which is shown in Figure 9, where a linear relationship was round over the range of water flow rates under consideration. Of course, the measuring period in the latter case is longer and it usually takes about 10 minutes to generate each average value.

If the local density of the liquid is given at each point by $(1-\alpha)$, where α is the local void fraction, $(1-\alpha)$ represents the probability of the existence of a liquid phase in the mixture. Knowing that the density of the liquid is the same in single or in two-phase flow under adiabatic conditions, the constant of calibration in single phase flow may be profiled.

The liquid velocity will be determined finally by:

$$U_{L2P} = 11.639 \sqrt{\frac{\Delta P}{1-\alpha}} \qquad (1)$$

where U_{L2P}: liquid phase velocity (ft/sec).

ΔP : differential pressure given by the system of transducer XCO-080-50D and liquid isolator 0.020 in. (psid).

The equipment used to measure liquid phase velocity in cross-sectional planes is photographed in Figure 10.

The procedure and equipment for measuring the local void fraction has been previously described by Lakis and Trinh [28].

CHAPTER 4

EXPERIMENTAL RESULTS

4.1 Longitudinal distribution of average velocities in fully developed conditions

In order to facilitate the observation of flow development along the pipe, measured velocities at the pipe axis, U_c , are normalized with the mean velocities deduced from a given initial flow rate, U_o or with still superficial velocities.

Longitudinal distributions of velocity ratios U_{Lipc}/U_{Lo} and U_{Mc}/U_{Mo} are shown in Figures 11.a and 11.b for single phase and two-phase flows, respectively.

In single phase water flow, the normalized velocities tend to increase when the flow moves far downstream, in accordance with other previous experiments in which the development of a turbulent boundary layer normally accelerates fluid motion near pipe axis as far as axial location $z/D \simeq 100$.

In the presence of air bubbles, the normalized velocities are rather arbitrary from one flow volumetric quality to another. However, the violent mixing action almost completely disappears after $z/D = 110$ as shown in Figure 11.b.

By definition, the flow is supposed to be fully developed when:

* The longitudinal velocity distribution is unchanged. (single phase flow).
* The longitudinal void fraction distributions and mixture and phase velocities are statistically unchanged. (two-phase flow).

The latter can be understood as it the forms of void fraction and velocity profile remain relatively constant through out the pipe length.

The variation in liquid velocity profiles measured at 3 axial locations downstream is also given here in Figure 12, where measurements were taken at the highest liquid flow rate (≃5000 USGPM) with 11.6% and 26.4% as the chosen flow volumetric qualities.

Examination of velocity ratios in single and two-phase flows (Figures 11.a, 11.b, 12), and of void fraction ratios (Lakis and Trinh [28]), leads to the following conclusions:

- in single phase water flow, the flow is fully developed at axial location $z/D \simeq 100$.
- in two-phase flow, the flow is fully developed at axial location $z/D \geq 100$.

4.2 Distribution of continuous phase velocities

In a gas-liquid flow with liquid predominating, the initial liquid flow rate, U_{L_0}, plays an important role in producing turbulence and phase separation, and then local conditions of flow. Because of the importance of the use of the same measurement equipment in both single and two-phase flows, we will present first the verification of velocity distribution in both cross-sectional planes in two-phase flow.

4.2.1. Average velocity distribution laws in single phase flow

Measurements of velocity in single phase water flow may be verified by referring to the existing lws distinguishing the flow in a two regions: the core region and the small region right at the pipe wall.

In the core region, the big vortex lengthened in the axial direction controls almost all of the pipe cross-section, and the small vortexes formed within the big one reduce, next to a smaller stirring towards the pipe wall, fluid particles poor in energy. the intensity of the turbulence is almost unchanged and it is supposed that the turbulent viscosity is practically constant.

In the neighboring region of the wall, the flow is influenced by the viscosity and nature of the wall.

The principal product of turbulent energy is related to the pressure drop. Experiments in the past have shown that the ratio of average velocity to friction velocity, U/u*, does not depend on pipe radius, and that the low of the wall can be applied. In other regions, the distribution of the ratio $(U_{\text{ℓ}}-\bar{U})/u^*$ no longer depends on the nature of the wall and hardly at all on the viscosity, and the velocity defect law may be applied.

At a high Reynolds number, experiments have also indicated that there is a "recovery zone" where the two laws mentioned above are simultaneously applied. In this zone, the velocity distribution obey a logarithmic or universal law.

*Power law:

The determination of velocity distribution in turbulent flow is normally based both on logical hypothesis and experimental verification. In fully developed turbulent flow, the time-averaging velocity is unvaried with radial positions. The independent variables which are supposed to affect the velocity are: fluid density, dynamic viscosity of fluid, pipe diameter, radial position pipe wall roughness and average wall shear stress. Experiments by Nikuradse in water flow have demonstrated that the velocity profile may be approximated by a power law.

Experiments performed in this study agree very well and the final results of regression analysis are finally:

$$\frac{U}{U_{\mathcal{E}}} = (1 - |\, 2y^* - 1 \,|)^{0.071} \qquad (2)$$

(Re = $2*10^4$, arithmetic mean deviation = -1.3%, standard deviation = 0.2 %).

where U :time-averaging liquid velocity.

$U_{\mathcal{E}}$:liquid velocity at pipe axis.

y* :y/D, normalised radial position measured from pipe wall.

* Velocity defect law:

The effect of viscosity on flow is noticeable only in the near wall region where the velocity gradient is much greater than that near the pipe axis, while the wall roughness which affects the friction velocity, u*, for a given flow rate has a slight influence on the flow near the pipe axis. It may be supposed that the difference, $u_{max} - u$, depends uniquely on radial position, as:

$$\frac{U_{max} - U}{u^*} = A_1 \log_{10} \left(\frac{R}{y}\right)$$

where U_{max}: maximum velocity attained at pipe axis = U_c

U : local liquid velocity

U^* : friction velocity ($=\sqrt{\tau_p/l_L}$)

R : Pipe radius

Y : distance measured from pipe wall.

A_1 : unknown constant.

The wall shear stress is determined either by measured pressure drop or existing friction coefficient correlations. Our experimental results unable us to obtain:

$$\frac{U_c - U}{u^*} = 4.85 \log_{10} \frac{1}{1 - |2y^* - 1|} \qquad (3)$$

(Re = $2*10^4$, arithmetic mean deviation = 19.4 %, standard deviation = 4%).

* Universal distribution of velocities (in the neighborhood of the smooth wall, high Re)

The experimental works treating the case where the pipe radius has no effect on the velocity near the wall for very high Reynolds number - velocity whose average in the time at the same radial position depends only on τ_w, ρ and μ - have shown that the distribution of the velocity may be predicted by a "logarithmic profile" such that:

$$\frac{U}{u^*} = A \ln \eta + B$$

where

$$\eta = \frac{(1 - |2y^* - 1|\, Ru^*}{\nu}$$

ν : kinematic viscosity of fluid;

U : local velocity

u^* : friction velocity ($= \sqrt{\tau_w/\rho}$)

R : pipe radius

A and B are determined by linear regression such that:

$$\frac{U}{u^*} = 2.07 \ln \eta + 6.42 \qquad (4)$$

(Arithmetic mean deviation = -5.8%, standard deviation = 0.2%)

* Others:

In integrating expression (3) over the pipe cross-section, the average velocity of flow is obtained in the term:

$$\bar{U} = U_{\ell} - au^*$$

where:

$\bar{U}$: average velocity in the cross-section;

$U_{\mathfrak{C}}$: measured velocity at the centre line pipe.

u*: friction velocity.

a : unknown constant

The constant "a" is determined empirically, from where

$$\bar{U} = U_{\mathfrak{C}} - 3.82\ u^* \qquad (5)$$

(Arithmetic mean deviation = 1.4 % standard deviation = 7.6 %).

Rewriting (3) in the form:

$$\frac{U_{\mathfrak{C}}}{u^*} = \frac{U}{u^*} + 2.11\ \ln\ (1 - |2y^* - 1|)$$

we obtain, by substituting U_c / u^* in (4):

$$\frac{U_{\mathfrak{C}}}{u^*} = 2.11\ \ln \frac{Ru^*}{\nu} + 6.42 \qquad (6)$$

and by substituting (6) in (5):

$$\frac{U}{u^*} = 2.11 \ln \frac{Ru^*}{\nu} + 2.60 \qquad (7)$$

A comparison of the principal laws (Equations (2), (3) and (4)) with the literature (Schlichting [32]) is given in figure 13.

4.2.2 Cross-sectional distribution of liquid velocities in two-phase gas-liquid flow

4.2.2.a Transversal plane:

By supposing that the flow is stationary and ergodic, substitution of the average values of liquid phase dynamic pressure, ΔP, and the void fraction, α, at a radial position, y/D, in Equation (1) gives the average velocity of this phase, U_{L2P}.

Liquid phase velocity profiles in the transversal plane are shown in Figure 14.a. The profiles of normalised velocity, U_{L2P}/U_{L2Pc}, with a different flow volumetric quality, X_o, and different measurement stations, z/D, are also shown in Fig. 1.5.a and 1.5.b respectively. U_{L2Pc} is the average velocity of the liquid phase measured at the pipe axis.

The profile is more or less uniform at the beginning and becomes more and more asymmetrical as Z/D lengthens.

The asymmetry remains unchanged, even while the separation of the phases is in equilibrium with the diffusion rate in the entrained phase.

For a constant water flow rate, every increase in the injected air flow rate leads to an acceleration of the liquid phase in the upper part of the pipe, especially in the passages where there exists a strong concentration of void fraction. This displacement is, however, less rapid in the other half, particularly at the bottom of the pipe, where the order of size is smaller than that for a simple phase when the air flow rate is sufficiently low, and nearly equal for high injected air flow rates.

As the flow rate increases, acceleration is generally more important in the upper part of the pipe. This observation was also done by Ohba and coll. [11] in the study of a vertically ascending flow, where the bubbles are concentrated much more at the periphery of the pipe as air flow rate increases.

At a constant air flow rate, the increase of the water flow rate always accelerates the liquid phase.

For the low flow rates, the profiles measured before Z/D = 90 may be calculated (or evaluated) by a power law; beyond this distance, its form resembles that of the void fraction.

4.2.2.b Radial plane:

Liquid phase velocity distribution in the radial planes is uniform throughout the pit cross-section, as illustrated in Fig. 14.b.

In this place, the separation of phases by gravity has no influence on the determination of the parameter profiles only the turbulent diffusion of the entrained phase affects the homogeneity of the phase distribution, and the void fraction profile is therefore uniform and affects that of the phase velocity.

Although the void fraction has a tendency to disperse toward the wall when the flow rate increases, the difference between values near the wall and those near the pipe axis are not sufficiently important for the acceleration of the bubbles to affect the liquid velocity near the pipe axis.

The void fraction distribution, α, being nearly constant, the liquid velocity increases like that of a simple phase. The distribution form may be approximated by a power law as in the case of a vertical flow (Serizawa and al. [9], Ohba and coll. [11]).

If the characteristics of the profile (U/U_c for example) are compared with those of a simple phase, the difference is very small, which agrees particularly well with the results of Kozmienko and coll. [29]. (Re = 13400), where the velocities are determined by the electrochemical method, and the exponent is situated between 1/6 and 1/7 (Fig. 16).

CHAPTER 5

PREDICTION OF LIQUID PHASE VELOCITY IN DISPERSED BUBBLES FLOW

5.1 Proposed correlation

As has been seen, liquid phase velocity profiles may be approximated by a power law, an approach which has been employed by several researchers. The analysis of velocity profiles in the proceeding section permits the deduction of the relationship $U_{L2P} = f(X_o, \alpha)$, in which the void fraction, α, is already a function of the flow volumetric quality, X_o, and the radial position, y/D.

Approximation by the power law does not seem valid except in the radial plane where profile symmetry exists. In addition, the prediction of the liquid phase velocity of a predominatly liiquid flow may be more direct and easier to achieve, if the liquid velocity of a simple phase is considered as an explicit variable in the correlation.

In order to verify this hypothesis, the ratio between the local liquid velocities of a two-phase flow and those of a simple phase are expressed in terms of void fraction, as illustrated in Fig. 17 where we note the existence of a linear dependence between the ratios of velocities U_{L2P}/U_{L1P} and void

franction α.

The linear regression gives a relation of the form:

$$\frac{U_{L2P}}{U_{L1P}} = 1 + 0.842\alpha$$

This correlation is valid for all the values of α, $0 \leq \alpha \leq 0.5$. The estimated values and the experimental results are compared in figure 18 (arithmetic deviation = 1.2%, standard deviation = 1.1%).

5.2 Numerical analysis

The force balance which acts on the liquid phase of a statistically permanent flow permits the obtaining of the equations of movement of this phase whose radial gradient of velocity in the liquid phase is related to the eddy diffusivity of liquid and the interaction stress between the two phases.

The profile of the shear stress, τ_{int}- void fraction function, of the radial position of the wall shear stress -is obtained by calculating a numerical integral over the pipe diameter. Furthermore, in the case where the static pressure gradient is constant, the simplified expression is obtained for a fully developed flow.

According to Sato and Sekoguchi [13], the shear stress of the liquid phase may be separated into two parts: one corresponding to the components of velocity due to the inherent turbulence of the liquid only, the other a velocity component givent by the supplementary turbulence of liquid resulting in the agitatin of the bubbles.

In using the expression of the eddy diffusivity of the liquie, ε, proposed by Travis et al. [30] for a simple phase flow, where ε is calculated in the case of two-phase flow by $(1-\alpha)\varepsilon$, where $(1-\alpha)$ represents the probability of the presence of a liquid phase at a given point.

As was the case with τ_{int} , the liquid phase velocity profile is obtained in adimensional form.

5.2.1 Equations of motion for two-phase dispersed bubbles flow

5.2.1.a Unsteady flow

The governing equation for an unsteady two-phase dispensed flow may be written as (Trinh [20]):

Gas:

$$@r: \; -\frac{d}{dz}\int_0^r \alpha P_M \, 2\pi r dr + 2\pi r \tau_{int}$$

$$= \rho_g u_g \frac{du_g}{dz}\int_0^r \alpha \, 2\pi r dr + \rho_g \frac{\partial u_g}{\partial t}\int_0^r \alpha \, 2\pi r dr$$

$$+ \rho_g (u_g - u_L) \cdot \frac{d}{dz}(U_g - u_L) \cdot \int_0^r \alpha \, 2\pi r dr$$

$$+ \rho_g \frac{\partial}{\partial t}(u_g - u_L) \cdot \int_0^r \alpha \, 2\pi r dr \qquad (9.1)$$

$$@R: \; -\frac{d}{dz}\int_0^R \alpha P_M \, 2\pi r dr - 2\pi R \tau_{wg}$$

$$= \rho_g u_g \frac{du_g}{dz}\int_0^R \alpha \, 2\pi r dr + \rho_g \frac{\partial u_g}{\partial t}\int_0^R \alpha \, 2\pi r dr$$

$$+ \rho_g (u_g - u_L) \cdot \frac{d}{dz}(U_g - u_L) \cdot \int_0^R \alpha \, 2\pi r dr$$

$$+ \rho_g \frac{\partial}{\partial t}(u_g - u_L) \cdot \int_0^R \alpha \, 2\pi r dr \qquad (9.2)$$

Liquid:

$$@r: \; -\frac{d}{dz}\int_{o}^{r}(1-\alpha)\,P_M\,2\pi r dr - 2\pi r\tau_{int}$$

$$= \rho_L\,u_L\,\frac{du_L}{dz}\int_{o}^{r}(1-\alpha)\,2\pi r dr + \rho_L\,\frac{\partial u_L}{\partial t}\int_{o}^{r}(1-\alpha)\,2\pi r dr$$

$$+ \rho_L\,(u_L - u_\Theta)\cdot\frac{d}{dz}(U_L - u_\Theta)\cdot\int_{o}^{r}(1-\alpha)\,2\pi r dr$$

$$+ \rho_L\,\frac{\partial}{\partial t}(u_L - u_\Theta)\cdot\int_{o}^{r}(1-\alpha)\,2\pi r dr \qquad (10.1)$$

$$@R: \; -\frac{d}{dz}\int_{o}^{R}(1-\alpha)\,P_M\,2\pi r dr - 2\,\pi R\tau_{w2p}$$

$$= \rho_L\,u_L\,\frac{du_L}{dz}\int_{o}^{R}(1-\alpha)\,2\pi r dr + \rho_L\,\frac{\partial u_L}{\partial t}\int_{o}^{R}(1-\alpha)\,2\pi r dr$$

$$+ \rho_L\,(u_L - u_\Theta)\cdot\frac{d}{dz}(U_L - u_\Theta)\cdot\int_{o}^{R}(1-\alpha)\,2\pi r dr$$

$$+ \rho_L\,\frac{\partial}{\partial t}(u_L - u_\Theta)\cdot\int_{o}^{R}(1-\alpha)\,2\pi r dr \qquad (10.2)$$

5.2.1.b Steady flow

If the flow is statistically steady, the time average accelaration of the fluid equals zero, the forces acting on an element of fluid must be in balance, and we then obtain:

Gas:

$$@r:- \frac{d}{dz}\int_o^r \alpha P_M\, 2\pi r dr + 2\pi r\tau_{int} = \rho_G \int_o^r \alpha 2\pi r dr \left[u_G \frac{du_G}{dz} + u_{GL} \frac{du_{GL}}{dz}\right] \quad (11.1)$$

$$@R:- \frac{d}{dz}\int_o^R \alpha P_M\, 2\pi r dr + 2\pi r\tau_{wG} = \rho_G \int_o^R \alpha 2\pi r dr \left[u_G \frac{du_G}{dz} + u_{GL} \frac{du_{GL}}{dz}\right] \quad (11.2)$$

Liquid:

@r:

$$-\frac{d}{dz}\int_o^r (1-\alpha) P_M\, 2\pi r dr - 2\pi r\tau_{int} = \rho_L \int_o^r (1-\alpha) 2\pi r dr \left[u_L \frac{du_L}{dz} + u_{LG} \frac{du_{LG}}{dz}\right] \quad (12.1)$$

@R:

$$-\frac{d}{dz}\int_o^R (1-\alpha) P_M\, 2\pi r dr - 2\pi r\tau_{wall} = \rho_L \int_o^R (1-\alpha) 2\pi r dr \left[u_L \frac{du_L}{dz} + u_{LG} \frac{du_{LG}}{dz}\right] \quad (12.2)$$

5.2.2 Liquid phase velocity in one dimensional horizontal and steady flow

5.2.2.a Statistically steady and partially developed turbulent flow

Concerning the liquid phase, we consider only equations (12.1) and (12.2). The sum of (12.1) $*-\int_J (1-\alpha)\ 2\pi r dr$ and (12.2) $*\int_J (1-\alpha)\ 2\pi r dr$ yields:

$$\tau_{int} = -\frac{1}{r}\frac{d}{dz}\left[\int_o^r (1-\alpha)\ P_M\ r dr\right]$$

$$+\frac{1}{r}\frac{d}{dz}\left[\int_o^R (1-\alpha)\ P_M\ r dr\right]\cdot\frac{r^2 - 2\int_o^r \alpha r dr}{R^2 - 2\int_o^R \alpha r dr}$$

$$+\tau_{w2P}\frac{R}{r}\cdot\frac{r^2 - 2\int_o^r \alpha r dr}{R^2 - 2\int_o^R \alpha r dr}$$

Furthermore, from Equation (A.6):

$$\frac{du_L}{dr} = -\frac{\tau_{int}}{\rho_L\ \varepsilon_{2P}} = -\frac{\tau_{int}}{\varepsilon_{2P}/(1/\rho_L)} \qquad (13)$$

Multiplying Equation (13) by $(1/\tau_{w2P})$ $(1/\tau_{w2P})$ and define

ρ:

$$\frac{\tau_{w2P}}{\rho_L} = u^*_{2P} \quad , \quad \frac{\varepsilon_{2P}}{R_M u^*_{2P}} = \varepsilon^*_{2P}$$

$$\frac{u_L}{u^*_{2P}} = O_L \quad , \quad \frac{(1-\alpha)P_M}{\rho_L u^*_{2P}} = P^*_L$$

$$\frac{r^2 - 2\int_0^r \alpha r dr}{R^2 - 2\int_0^R \alpha r dr} = \frac{r^{*2} - 2\int_0^{r^*} \alpha r^* dr^*}{R^{*2} - 2\int_0^1 \alpha r^* dr^*} \qquad (14)$$

where: $r^* = \frac{r}{R}$, $Z^* = \frac{Z}{L}$, $dr = R dr^*$, $dZ = L dZ^*$

The liquid phase velocity finally becomes:

$$\frac{dO_L}{dr^*} = \frac{1}{\varepsilon^*_{2P}}\left[-\frac{1}{r} \cdot \frac{r^{*2} - 2\int_0^{r^*} \alpha r^* dr^*}{1 - 2\int_0^1 \alpha r^* dr^*} + \frac{R}{Lr^*}\frac{d}{dZ^*} \cdot \left\{ \int_0^{r^*} P^*_L r^* dr^* - \int_0^1 P^*_L r^* dr^* - \int_0^1 P^*_L r^* dr^* \frac{r^{*2} - 2\int_0^{r^*} \alpha r^* dr^*}{1 - 2\int_0^1 \alpha r^* dr^*} \right\} \right] \qquad (15)$$

5.2.2.b Statistically steady and fully developed turbulent flow

If the flow is fully developed all variable relative to fluid (velocity, pressure, void fraction, etc.) do not change in the flow direction. This proposition implies that, from equation (15):

$$\frac{d}{dZ^*}\,[\ldots\ldots\ldots] = 0 \qquad (16)$$

We then have:

$$\boxed{\frac{d\phi_L}{dr^*} = \frac{1}{\varepsilon^*_{2P}}\left[-\frac{1}{r^*}\cdot\frac{r^{*2} - 2\int_0^{r^*}\alpha r^*\,dr^*}{1 - 2\int_0^1 \alpha\, r^*\,dr^*}\right]} \qquad (17)$$

5.2.3 Shear stress in two phase flow one dimensional horizontal steady flow

5.2.3.a Statistically steady and partially developed turbulent flow

Substituting Equation (14) into Equation (13) we obtain:

$$\boxed{\tau^*_{int} = -\varepsilon^*_{2P}\,\frac{d\phi_L}{dr^*}} \qquad (18)$$

where:

$$\tau^{*}_{int} = \frac{\tau_{int}}{\rho_L u^{*2}_{2p}}$$

and: $\frac{d\phi_L}{dr^*}$ is given by Equation (15)

5.2.3.b Statistically steady and fully developed turbulent flow

Performing the same operation as above with Equations (14), (16) and (13), we obtain:

$$\boxed{\tau^{*}_{int} = -\varepsilon^{*}_{2p} \frac{d\phi_L}{dr^*}} \qquad (19)$$

where: $\frac{d\phi_L}{dr^*}$ is given by Equation (17)

5.4.2. Numerical solution of liquid velocity profile

5.2.4.a Distribution of liquid velocity in two-phase flow

This presents a mathematical development of a statistically steady and fully developed flow. Rewriting Equation (17) in the other form:

$$d\phi_L = \frac{1}{b\ (1-\alpha)} \cdot \frac{a_i - r^{*2}}{r^*\ (-0.1790\ r^{*4} + 0.1192 r^{*2} + f_i)}\ dr^* \qquad (20)$$

where:

$$\varepsilon^{*}_{2F} = (1-\alpha)\ (-0.1790\ r^{*4} + 0.1192\ r^{*2} + f_i)$$

$$f_i = \frac{\nu_L}{Ru^{*}_{2F}} + \frac{K''\bar{r}_\Theta\ \bar{U}_\Theta\ \alpha}{Ru^{*}_{2F}} + 0.06$$

$$a_i = 2 \int_0^{r^*} \alpha\ r^*\ dr^*$$

$$b = 1 - 2 \int_0^{1} \alpha r^*\ dr^*$$

According to the steplike arrangement shown in Figure 18.b,

We obtain, from the integration of Equation (20) in the new coordinates:

$$r^* = |\ 2y^* - 1\ |$$

where:

$$y^* = \frac{Y}{D}$$

$$\int_{\phi_{L\,i-1}}^{\phi_{L\,i}} d\phi_L = \frac{1}{b\ (1-\alpha)} \left[\int_{r^*_i}^{r^*_{i+1}} \frac{a_i\ dr^*}{r^*\ (Ar^{*4}+Br^{*2}+C_i)} - \int_{r^*_i}^{r^*_{i+1}} \frac{r^*\ dr^*}{Ar^{*4}+Br^{*2}+C_i} \right]$$

where: $A: = -0.1790$, $B = 0.1192$, $C_i = f_i$

We obtain, finally, for filly developed flow:

$$\phi_{Li}=\phi_{Li-1} + \frac{1}{1-\alpha_i}\frac{a_i}{4bC_iF_i}\left[F_i\,(H_{i+1}-H_i) - (G_{i+1}-G_i)\left(\frac{2C_i}{a_i} + 0.1192\right)\right] \qquad (22)$$

where: $i = 1, 2 \ldots n-1$

n: number of points (= number of radial positions in half channel (include the centre line position) + 1)

$$a_i = 2\sum_{k=1}^{i}\frac{\alpha_k}{2}\left(|2y^*_{k+1}-1|^2 - |2y^*_{k+1}-1|^2\right)$$

$$b = 1 - 2\sum_{k=1}^{n-1}\frac{\alpha_k}{2}\left(|2y^*_{k+1}-1|^2 - |2y^*_{k+1}-1|^2\right)$$

$$C_i = \frac{\nu_L}{Ru^*_{2P}} + \frac{K''\overline{F}_G\overline{U}_G\alpha_i}{Ru^*_{2P}} + 0.06 \qquad (23)$$

$$Fi = (0.0142 + 0.7160\,C_i)\,0.5$$

$$G_{\substack{(i)\\(i+1)}} = \ln\left|\frac{-0.3580\,|2y^*_{\substack{(i)\\(i+1)}}-1|^2 + 0.1192 - F_i}{-0.3580\,|2y^*_{\substack{(i)\\(i+1)}}-1|^2 + 0.1192 + F_i}\right|$$

$$H_{(i)}^{(i+1)} = \ln \left| \frac{|2y^{*}_{(i)} - 1|^{4}}{(i+1)} \right| \Bigg/ \left| - 0.1790 \; |2y^{*}_{(i)} - 1|^{4} + 0.1192 |2y^{*}_{(i)} - 1|^{2} + C_i \right|$$
$$(i+1) \qquad\qquad (i+1)$$

$$\phi_L = \frac{U_L}{U^{*}_{2P}}$$

5.2.4.b Distribution of liquid velocity in single phase flow

Making $\alpha_i = 0$, we have, according to Equation (23),

$$\boxed{\phi_{L1Pi} = \phi_{L1P_{i+1}} + \frac{1}{2F_i} \; (G_i - G_{i+1})} \qquad (24)$$

with $$\phi_L = \frac{U_{L1P}}{U^{*}_{1P}}$$

$$G_{(i)}^{(i+1)} = \ln \left| \frac{- 0.3580 \; |2y^{*}_{(i)} - 1|^{2} + 0.1192 - F_i}{(i+1)} \right| \Bigg/ \left| - 0.3580 \; |2y^{*}_{(i)} - 1|^{2} + 0.1192 - F_i \right|$$
$$(i+1)$$

$$F_i = (0.0142 + 0.7160 \; C_i) \; 0.5$$

$$C_i = \frac{v_L}{Ru^*_{ip}} + 0.06$$

Comparison of the numerical model and experimental results is given in Figures (20) and (21) for velocity and shear stress distributions in two-phase flow, respectively.

Graphs indicate that the numerical model offers better results in the radial plane.

In the transversal plane, numerical results are still comparable at low air flow rates; discrepancies start to appear when flow volumetric quqality $X_v \geq 20\%$.

In order to obtain better results in the transversal plane, it will be suggested that analysis of flow in two dimensions and consideration of lift, drag, and mass forces be galien into account in the future formulations.

CHAPTER 6

CONCLUSION

Local liquid phase velocity may be determined in several ways; among them, the use of the liquid isolator (or bubble eliminator) with a miniature pressure transducer or even the Pitot tube to facilitate the measurement and interpretation of impact pressure in two-phase flow. Its design takes into consideration minimum perturbation at local measuring points, maximum efficiency in eliminating bubbles and a reasonable mesuring period. Liquid phase velocity may then be deduced knowing local liquid density. the reliability of this indirect method depends essentially on calibration procedure.

Experimental results indicate, in a raidal plane, that the velocity profiles behave like those of single phase flow for various chosen values of flow volumetric quality. It was also found that their form is quite similar in both small and large diameter pipes.

In the transversal plane, the asymmtry of the profiles appears from $X \geq 12$ % and remains unchanged from axial location $z/D \geq 100$ where the two-phase flow is assumed to be completely developed; X_ω is the flow volumetric quality.

The velocity of the continuous phase (liquid) and the void fraction strongly influence phase distribution in the pipe. The ratio of velocity in two-phase flow to that of single phase was found to be a linear function of the void fraction, in the range of $0 < X_v < 0.5$.

Based on the assumptions of turbulent shear stress in bubbly flow given by Sato and Sekoquchi [13], a numerical model was developed to predict the distributions of liquid velocity and shear stress the present in despersed bubbles flow. the numerical model includes eddy diffusivity relationship in single phase water flow proposed by Travis et al. [30], measured values of pressure drop, mean local velocity of bubbles, mean bubble diameter and local void fraction in fully developed flow.

Numerical results agree well with measurements in radial plane. Discrepancies in compared values in the transversal plane were noted at flow volumetric quality $X \geq 20$ %. Lift, drag, mass forses, etc... seem to be important in horizontal flow and suggested taht these be included in the next step in the numerical analysis.

REFERENCES

[1] JEPSEN, J.C., RALPH, J.L. (1970)
"Hydrodynamic Studies of Two-Phase Upflow in Vertical Pipelines".
Proc. Instn. Mech. Engrs., (1969-70), vol. 184, Part 3C. Communication 20, p. 154-165.

[2] KINOSHITA, T., MURASAKI, T. (1969)
"On a Stochastic Approach to the Pulsating Phenomena in the Two-Phase Flow".
ISME, vol. 12, no. 52, p. 819-826.

[3] SERIZAWA, A., KATAOKA, T., MICHIYOSHI, I. (1973)
"Turbulent Structure of Air-Water Bubbly Flow (1) and (11)".
Proc. 1973 Ann. Meet. At. Energy Soc. Japan.

[4] MITCHELL, J., HARATTY, T.J. (1966)
"A Study of Turbulent at a Wall Using an Electrochemical Wall Shear Stress Meter".
J. Fluid Mech., vol. 26, p. 199-221.

[5] KOZMIENKO, B.K., NAKORIAKOW' W.E., BURDUKOW, A.P., KOWALSKI, J., SLIWICKI, E. (1976).
"Velocity Profile of the Liquid Phase in a Two-Phase Flow with Bubble Structure". (in Polish).
Polska Akademia Nauk, Prace Instytutu Maszyn Przeplywowych, p. 23-29.

[6] ALIA, P., CRAVAROLO, L., HASSID, A., PETROCCHI, E. (1968)
"Phase and Velocity Distribution in Two-Phase Adiabatic Annular Dispersed Flow".
Energia Nucleare, vol. 15, no. 4, April 1968, p. 242-254.

[7] DELHAYE, J.M. (1969)
"Hot Film Anemometry in Two-Phase Flow".
Proc. 11th Nat. ASME/AICHE Heat Transfer Conf. on two-phase Instr., Minneapolis (minnesota), p. 58-69.

[8] SERIZAWA, A., KATAOKA, I., MICHIYOSHI, I. (1975)
"Turbulent Structure of Air-Water Bubbly Flow I. Measuring Techniques".
Int. J. Multiphase flow, vol. 2, p. 221-233.

[9] SERIZAWA, A., KATAOKA, I., MICHIYOSHI, I. (1975)
"Turbulent Structure of Air-Water Bubbly Flow II. Local Properties".
Int. J. Multiphase flow, vol. 2, p. 235-246.

[10] GALAUP, J.P. (1975)
"Contribution à l'étude des méthodes de mesure en écoulement diphasique".
Thèse de Doctorat, Université de Grenoble.

[11] OHBA, K., KISHIMOTO, I., OGASAWARA, M. (1977)
"Simultaneous Measurement of Local Liquid Velocity and Void Fraction in Bubbly Flows Using a Gas Laser Part II. Local Properties of Turbulent Bubbly Flow".
Technol. Rep. Osaka Univ., vol. 27, Mars, no. 1358, p. 228-238.

[12] BROWN, R.W., GOMEZPLATA, A., PRICE, J.D. (1969)
"A Model to Predict Void Fraction in Two-Phase Flow".
Chemical Engineering Science, vol. 24, p. 1483-1489.

[13] SATO, Y., SEROGUCHI, K. (1975)
"Liquid Velocity Distribution in Two-Phase Bubble Flow".
Int. J. Multiphase flow, vol. 2, p. 79-95.

[14] BANKOFF, S.G. (1960)
"A Variable Density Single Fluid Model for Two-Phase Flow with Particular Reference to Steam-Water Flow".
J. of Heat Transfer, Trans. ASME, ser. C, vol. 82, Nov., p. 265-272.

[15] BROWN, F.C., KRANICH,. W.L. (1968)
"A model for the prediciton of velocity and void fraction profiles in two-phase flow".
AICHE, vol. 14, Sept., p. 750-758.

[16] KASCHEEV, V.M., MURANOV, YU. V. (1968)
"Calculation of Velocity Profile in Two-Phase Dispersed Annular Flow".
High Temperature, vol. 14, Sept. Oct., no.5, p. 901-907.

[17] LEVY, S. (1963)
"Prediction of Two-Phase Pressure Drop and Density Distribution from Mixing Length Theory".
J. of Heat Transfer, Trans. ASME, ser. C, vol. 85, May, p. 137-152.

[18] GORIN, A.V. (1978)
"Friction and the Velocity and Gas Content Profiles of a Turbulent Gas-Liquid Flow".
J. of Engineering Physics, vol. 35, Spet., no.3, p.1029-1036.

[19] LAKIS, A.A. (1978)
"Numerical Analysis of Wall Pressure Fluctuations in Two-Phase Flow".
Numerical methods in laminar and turbulent flow, 17tn 21st, Proc. of 5th Int. Cont., July, Univ. Col.Swansea, UK, p. 757-767.

[20] TRINH, N.D. (1986)
"Experimental and Numerical Predictions of Turbulent Two-Phase Flow Parameters".
Ph.D. Thesis, Ecole Polytechnique de Montréal, Univ. of Montreal, Québec, Canada.

[21] HALBRONN, G. (1951)
"Mesure des concentrations et des vitesses dans un courant mixte d'air et d'eau".
La Houille Blanche, Mai Juin, p. 394.

[22] GILL, L.E., HEWITT, G.F., HITCHEN, J.W. (1962)
"Sampling Probe Studies of the Gas Core in Annular Two-Phase Flow. Part 1. The Effect of Length on Phase Velocity Distribution".
AERE R, no. 3954.

[23] ZIGAMI, T., KATAOKA, I., SERIZAWA, A., MICHIYOSHI, I. (1974)
"Liquid Velocity Measurement in Two-Phase Flow Using a Pitot Tube".
Fall Meet. of the Atomic Energy Society of Japan, E. 13, p. 195.

[24] FINCKE, J.R., DEASON, V.A. (1978)
"Fluid Dynamics Measurements in Air-Water Mixtures Using a Pitot Tube and Gamma Densitometer".
ISA, ISDN 87664 407 8, p. 621-626.

[25] LAKIS, A.A., MOHAMED, S.S. (1979)
"Pitot Tube Measurements in Fully Developed Turbulent Dispersed Flow".
Multiphase Transport, Fundamentals, Reactor safety, Application. Eq. N. Veziroviu, vol. 5, April, p. 2605-2619.

[26] ANDERSON, G.H., MANTZOURANIS, B.G. (1960)
"Two Phase (Gas-Liquid) Flow Phenomena 11. Liquid Entrainment".
Chemical Engineering Science, vol. 12, no. 4, p. 233-242.

[27] SHIRES, G.L., RILEY, P.J. (1966)
"The Measurement of Radial Voidage Distribution in Two-Phase Flow by Isokinetic Sampling".
A.E.E.W., M 650.

[28] LAKIS, A.A., TRINH, N.D. (1988)
"Void Fraction in Highly Turbulent and Large Diameter Horizontal Pipe Flow".
Report no. EPM/RT 88, Ecole Polytechnique de Montréal, Québec, Canada.

[29] BURDUKOV, A.P., VALUKINA, N.V. (1975)
"Special Characteristics of the Flow of a Gas-Liquid Bubble Type Mixture with Small Reynolds Numbers".
Shurnal Prik. Mekh. Tech. Fiziki, no. 4, p. 137-141.

[30] TRAVIS, J.R., BURH, H.O., SESONSKE, A. (1971)
"A Model for Velocity and Eddy Diffusivity Distributions in Fully Turbulent Pipe Flow"
The Canadian J. of Chem. Eng., vol. 49, Feb., p. 14-18.

[31] REICHARDT, M.Z. (1951)
"Vollstandige Darstellung der Turbulenten Geschwindigkeitsverteilung in Glatten Leitungen".
Z. Angew. Math. U. Mech., vol. 31, p. 208-219.

[32] SCHLICHTING, H. (1968)
"Boundary Layer Theory".
McGray Hill Book Co. Inc., 6th edition.

[33] LAUFER, J. (1954)
"The Structure of Turbulence in Fully Developed Pipe Flow"
Tech. Rep. Nat. Adv. Comm. Aero, wash, no. 1174.

[34] NIKURASE, J. (1932)
"GesetzmaBigheit der Turbulenten Stromung in Glatten Rohren, Forsch. Arb. Ing".
WES no. 356.

[35] VAN DRIEST, E.R. (1956)
J. Aero. Sci., vol. 23, p. 1007.

[36] DARCY, H. (1858)
"Recherche expérimenales relatives aux mouvemens de l'eau dans les tuyaux".
Mem. prés. à l'Académie des Sciences de l'Institut de France, vol. 15, p. 141.

[37] VON KARMAN, TH. (1921)
"Uber Laminare und Turbulente Reibung".
Z.A.M.M., vol. 1, p. 233-252.

[38] WIEGHARDT, K. (1946)
"Turbulente Grenzchnichten".
Gottinger Monographic, part B5.

APPENDIX A

TURBULENT SHEAR STRESS AND EDDY DIFFUSIVITY OF TWO-PHASE DISPERSED BUBBLES FLOW

A.1 Turbulent shear stress

Referring to figure 19.a, momentum equations of a horizontal flow in cylindrical coordinates may be written as:

z:

$$\bar{u}_z \frac{\partial \bar{u}_z}{\partial Z} + \bar{u}_r \frac{\partial \bar{u}_z}{\partial r} =$$

$$- \frac{1}{\rho_L} \frac{\partial \bar{P}}{\partial z} + \frac{1}{\rho_L} \frac{\partial}{\partial z} \left(\mu_L \frac{\partial u_z}{\partial z} - \rho_L \overline{u'^2_z} - \rho_L \overline{u''^2_z} \right)$$

$$+ \frac{1}{r\rho_L} \frac{\partial}{\partial r} \left(\mu_L r \frac{\partial \bar{u}_z}{\partial r} - \rho_L \overline{ru'_z u'_r} \quad \overline{\rho_L ru''_z u''_r} \right) \qquad (A.1)$$

r:

$$\bar{u}_z \frac{\partial \bar{u}_r}{\partial Z} + \bar{u}_r \frac{\partial \bar{u}_r}{\partial r} =$$

$$- \frac{1}{\rho_L} \frac{\partial \bar{P}}{\partial z} + \frac{1}{\rho_L} \frac{\partial}{\partial z} \left(\mu_L \frac{\partial \bar{u_z}}{\partial z} - \rho_L \overline{u'_r u'_z} - \rho_L \overline{u'_r u''_z} \right)$$

$$+ \frac{1}{r\rho_L} \frac{\partial}{\partial r} \left(\mu_L r \frac{\partial \bar{u}_r}{\partial r} - \rho_L \overline{ru'^2_r} - \rho_L \overline{ru''^2_r} \right) - \mu_L \frac{\bar{u}_r}{r^2} \qquad (A.2)$$

where: u_z: flow velocity in the axial direction

u_r: flow velocity in the radial direction

Considering the flow in the axial direction Z, the mean velocities are in the same direction and parallel to the Z axis; the equaation (A.1) is reduced to:

$$\frac{\partial}{\partial r} r \left(\mu_L \frac{\partial \bar{u}_z}{\partial r} - \rho_L \overline{u'_r u'_z} - \rho_L \overline{u''_L u_z} \right) = \frac{\partial \bar{F}}{\partial z} r \qquad (A.3)$$

Integration of equation (A.3) gives:

$$\left(\mu_L \frac{\partial \bar{u}_z}{\partial r} - \rho_L \overline{u'_r u'_z} - \rho_L \overline{u''_r u''_z} \right) = \int \frac{\partial \bar{F}}{\partial z} r dr + Const. \qquad (A.4)$$

Considering the force balance of an element of fluid and if $(1 - \alpha)$ represents the probability of the existence of a liquid phase at a point in the mixture, the local shear stress of the liquid phase is:

$$\tau_{L\omega} = (1 - \alpha) \left[\mu_L \frac{\partial \bar{u}_z}{\partial r} - \rho_L \overline{u'_r u'_z} - \rho_L \overline{u''_r u''_z} \right] \qquad (A.5)$$

Moreover, $\tau_{L\ominus}$ is still the Reynolds stress of the turbulent flow.

According to the Prandtl's mixing length theory, the local shear stress of the liquid phase can be expressed as:

$$\tau_{L\ominus} = (1 - \alpha)\ \rho_L \left[\nu_L + \varepsilon'_L + \varepsilon''_\ominus\right] \left| \frac{du_z}{dr} \right|$$

where: $\varepsilon'_L = \rho''^2 \dfrac{du_z}{dr} = -\dfrac{\overline{u'_r u'_z}}{du_z/dr}$ Eddy diffusivity of liquid phase.

$\varepsilon''_\ominus = \rho''^2 \dfrac{du_z}{dr} = -\dfrac{\overline{u'_r u'_z}}{du_z/dr}$ Eddy diffusivity of gas phase.

$(1 - \alpha)\ \rho_L\ \varepsilon'_L \dfrac{d\bar{u}_z}{dr}$:shear stress due to momentum exchange of liquid phase particles between two adjacent layers.

$(1 - \alpha)\ \rho_L\ \varepsilon''_\ominus \dfrac{d\bar{u}_z}{dr}$:shear stress due to momentum exchange of liquid phase particles between two adjacent layers, caused by gas phase fluctuation.

$(1 - \alpha)\ \rho_L\ \nu_L \dfrac{d\bar{u}_z}{dr}$:shear stress due to laminar liquid viscosity.

Therefore: $$\tau_{L\theta} = - \rho_L \, \varepsilon_{2P} \frac{d\bar{u}_z}{dr} \qquad (A.6)$$

where:

$\varepsilon_{2P} = (1 - \alpha)(\nu_L + \varepsilon'_L + \varepsilon''_\theta)$ Eddy diffusivity in a two phase flow. (A.7)

A.2 Evaluation of eddy diffusivity terms

A.2.1 Eddy diffusivity in simple phase flow

Taking the model for prediction of eddy diffusivity in fully developed turbulent isothermal single phase flow of Travis et al. [30] ($4*10^3 < Re < 5*10^4$), which is the modified Reichard's model [31] adapted to correspond to experience, we may, for the central region and for $Re \geq 2*10^4$ in this study, write:

$$\varepsilon^*_{1P} = \frac{\varepsilon_{1P}}{Ru^*_{1P}} \qquad (A.8)$$

where: $\varepsilon_{1P} = 0.1790 \, Ru^*_{1P} (1 - r^{*2}) (0.333 + r^{*2})$

$r^* = \frac{r}{R}$, r is measured from the pipe centre line.

$$u^*_{1P} = \sqrt{\frac{\tau_{w1P}}{\rho_L}} \quad , \quad \tau_{w1P} : \left[F/L^2\right] \quad , \quad \rho_L : \left[FT^2/L^4\right]$$

A.2.2 Eddy diffusivity in two-phase flow

If is known to be applicable for $4*10^3 < Re < 5*10^6$ we suppose that $\varepsilon'_L = \varepsilon_{1P}$ for $Re_{max} = 5*10^6$ where Re_{max} is calculated for liquid phase velocity, and the friction velocity U^*_{1P} is replaced by U* 2p, Equation (A.8) becomes:

$$\varepsilon'_L = 0.1790\ Ru^*_{2P}\ (1 - r^{*2})\ (0.333 + r^{*2}) \qquad (A.9)$$

The eddy diffusivity ε''_Θ is given by Sato and Sekoguchi [40] (air-water flow):

$$\varepsilon''_\Theta = K''\alpha\ \frac{\bar{d}_\Theta}{2}\ \bar{U}_\Theta \qquad (A.10)$$

where: K" : Unknown constant.

$\bar{d}_\Theta$: mean diameter (spae average) of bubbles across the pipe section.

$\bar{U}_\Theta$: mean local velocity of bubbles (space average).

α : void fraction.

Substituting Equations (A.9) and (A.10) and Equation (A.7), we obtain the eddy diffusivity if a two-phase flow in non-dimensional form:

$$\varepsilon^*_{2P} = (1-\alpha)\,(-0.1790\, r^{*4} + 0.1192\, r^{*2} + f_1) \qquad (A.11)$$

where:

$$f_1 = \frac{\nu_L}{Ru^*_{2P}} + \frac{K'' Fo\ \Omega_0\ \alpha}{Ru^*_{2P}} + 0.06$$

$$u^*_{2P} = \sqrt{\frac{\tau_{w2P}}{\rho_L}}$$

$$\varepsilon^*_{2P} = \frac{\varepsilon_{2P}}{Ru^*_{2P}}$$

$$r^* = \frac{r}{R}$$

AIR

T_G = 24°C ± 2°C, P_G = 50 psig, ρ_G = 0.255 lbm/ft^3

WATER

T_L = 19°C ± 2°C, P_L = 1 atm, ρ_L = 62.4 lbm/ft^3
ν_L = 1.088 * 10^{-5} ft^2/ sec.

Q (ft^3/min)	U (ft/sec)	X_o	Q_{Lo}(USGPM)	U (ft/sec)
76.6	4.03	.116	4373	30.74
73.8	3.88	.131	3666	25.77
147.6	7.76	.219	3940	27.69
209.8	11.03	.264	4373	30.74
202.2	10.63	.292	3666	25.77

$$X_o = \frac{Q_{Go}}{Q_{Go}+Q_{Lo}},\ Q_{Go} = 19.02 * U_{Go},\ Q_{Lo} = 142.26 * U_{Lo},\ \rho_G = \frac{2.698 * (PSIG)}{459.69 + °F}$$

ID = 7.625 in, Re_L(max) = 2 * 10^6, Mach(max)= 0.014 (<0.2, incompressible)

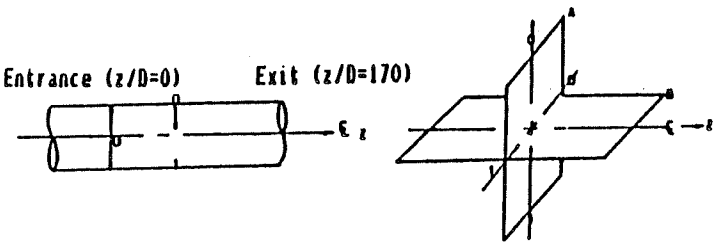

* 24 axial locations.
* 9 radial positions (tranversal plane A and radial plane B).

Table 1 Experimental conditions

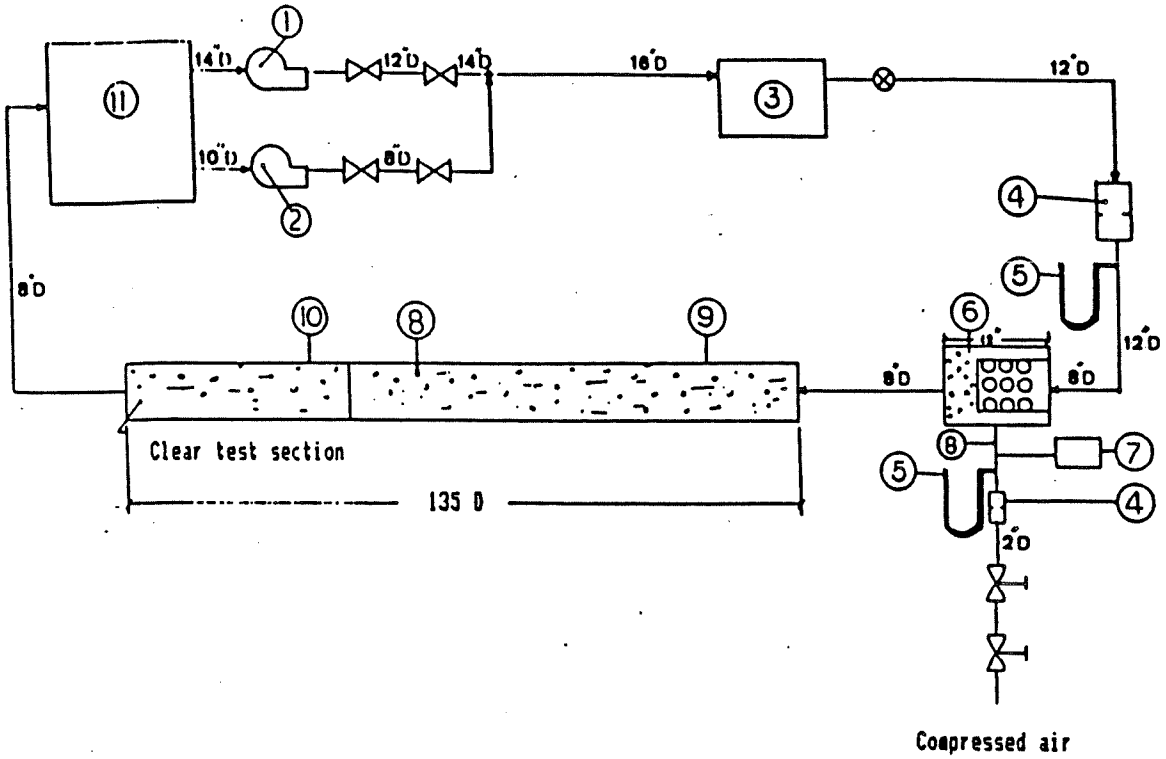

⧖ : monitoring control valve
⧖ : regulator of constant pressure
⊗ : manual control valve

1) Pump (150 HP).
2) Pump (75 HP).
3) Closed pressure vessel (45 psi).
4) Orifice meter.
5) Hg U-manometer.
6) Air-Water mixer.
7) Pressure gauge.
8) Thermometer.
9) Test section.
10) Measurement apparatus (Pitot, probe...)
11) Open reservoir tank

Figure 1 Horizontal test loop

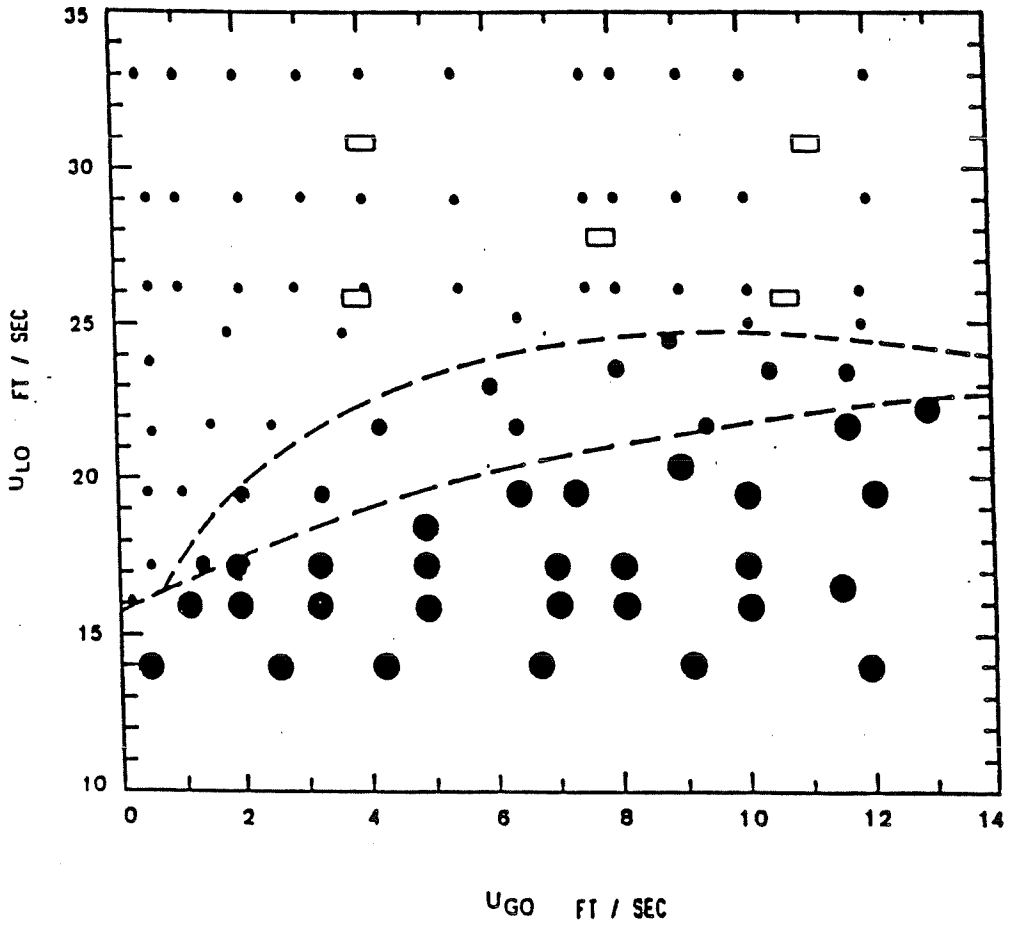

Figure 2 Flow map of horizontal air-water flow.
(8-in. nominal diameter, fully developed flow z/D = 130)

- Slug flow
- Dispersed slug waved flow
- Stratified-dispersed bubbles flow
- Values chosen for experimentation
- --- Transition zones.

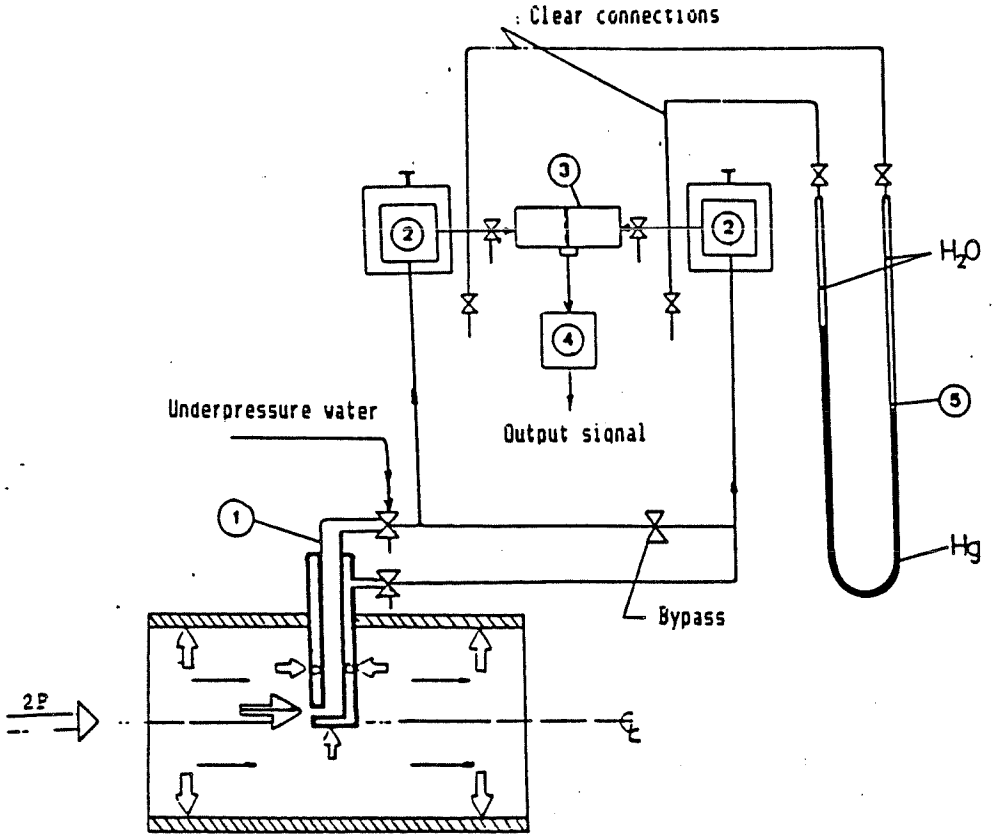

⇨ Statis pressure.
— Dynamic pressure.
⇨ Total pressure.

1) Pitot tube (model 310, SSI-TAYLOR, SYBRON CORP.).
2) Air purger.
3) Differential pressure transucer (CJVR-10PSI.S7N 1783).
4) Carrier modulator (model CJCD-3091, ser. 1795).
5) U-manometer.

Figure 3 Measurement of dynamic pressure in two-phase flow with Pitot tube and differential pressure transducer.

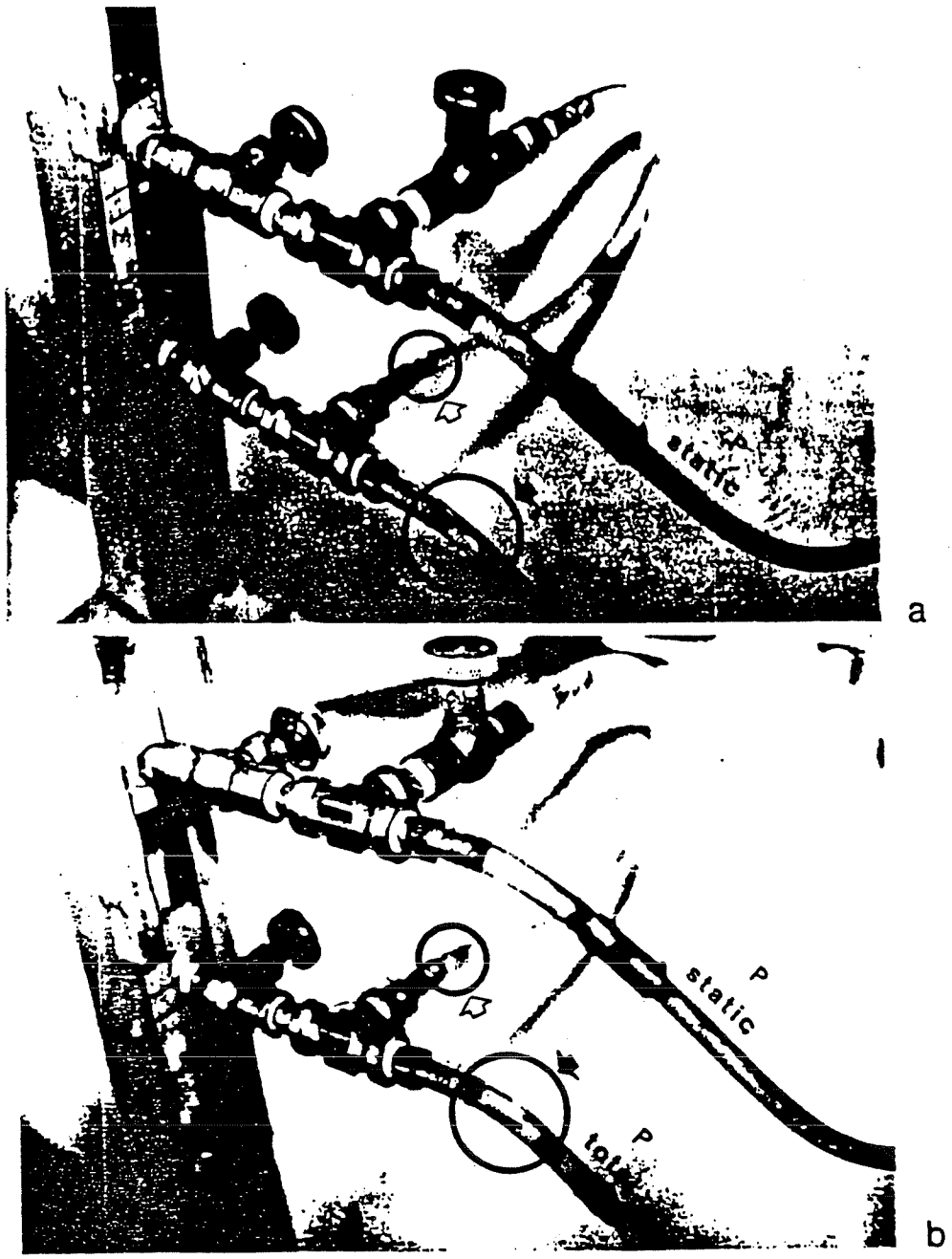

Figure 4 Presence of bubbles in static and total pressure connection tubes.
4.a At y/D = 0.238, X_o = 0.116, after ≅ 12 minutes.
4.b At y/D = 0.238, X_o = 0.282, after ≅ 07 minutes.

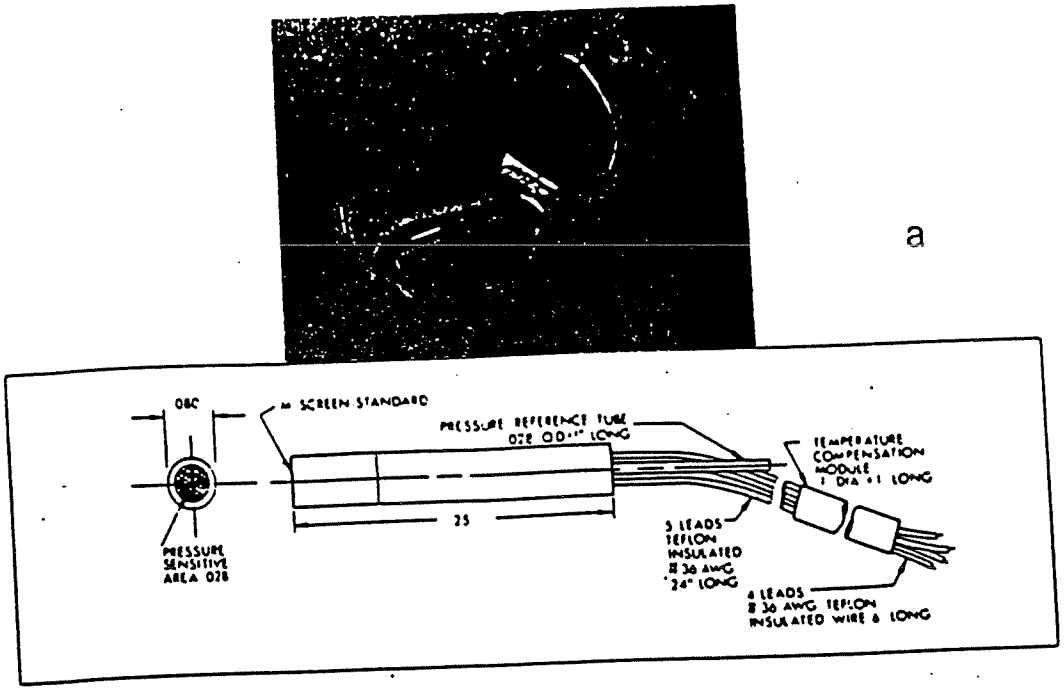

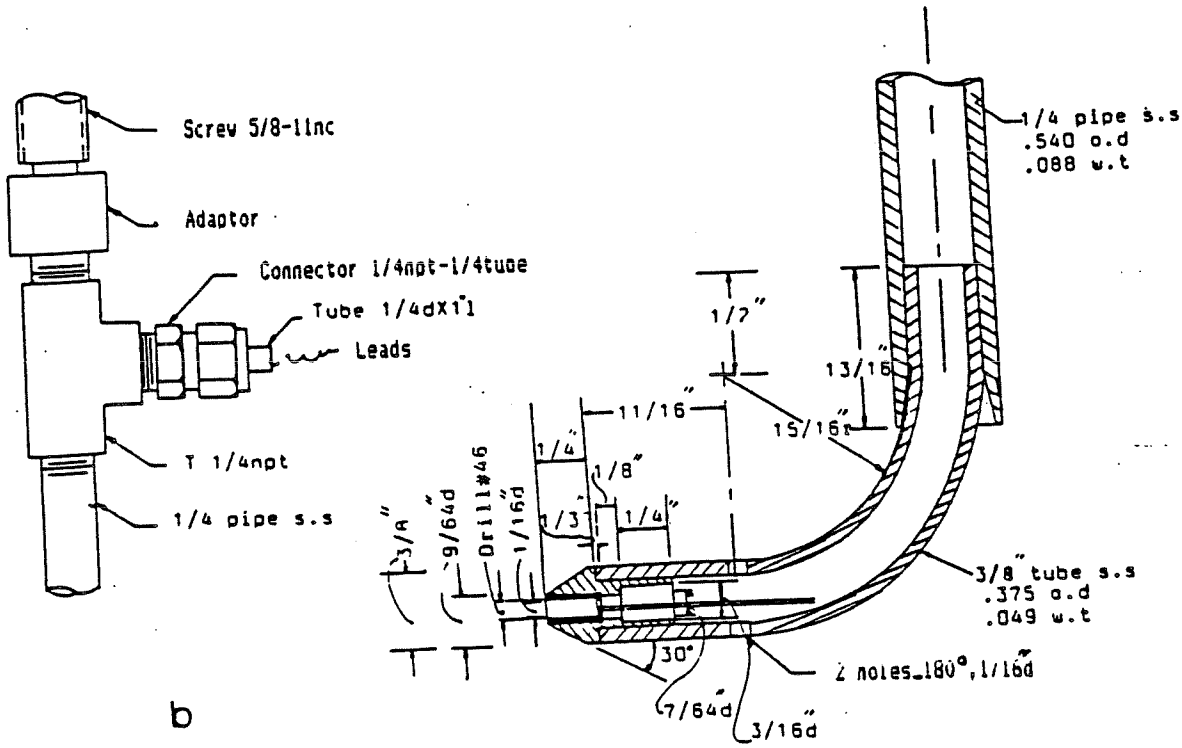

Figure 5 5.a Miniature differential pressure transducer XCQ-080-50D.
5.b Sketch of support of transducer XCQ-080-50D.

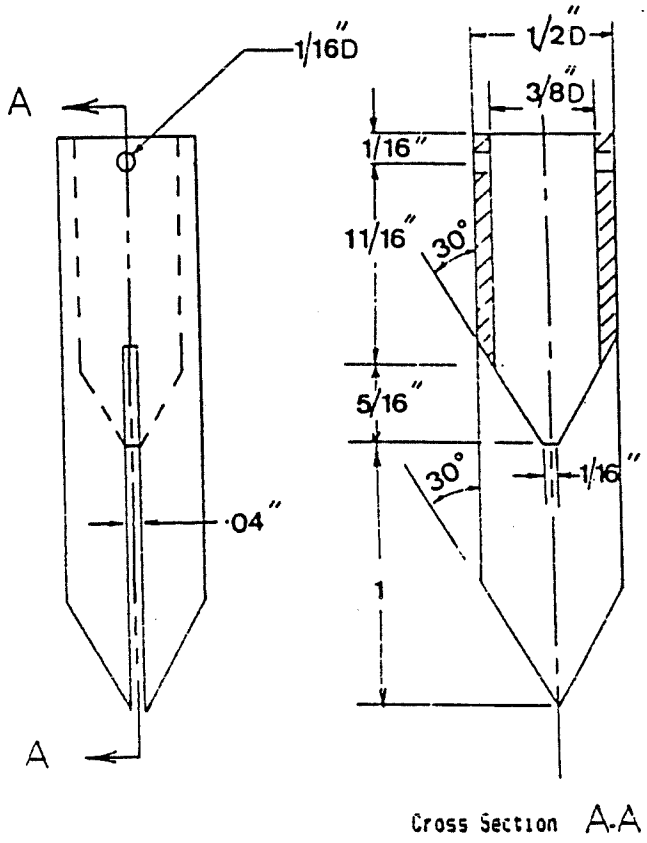

Figure 6.a Design of optimum liquid phase isolation

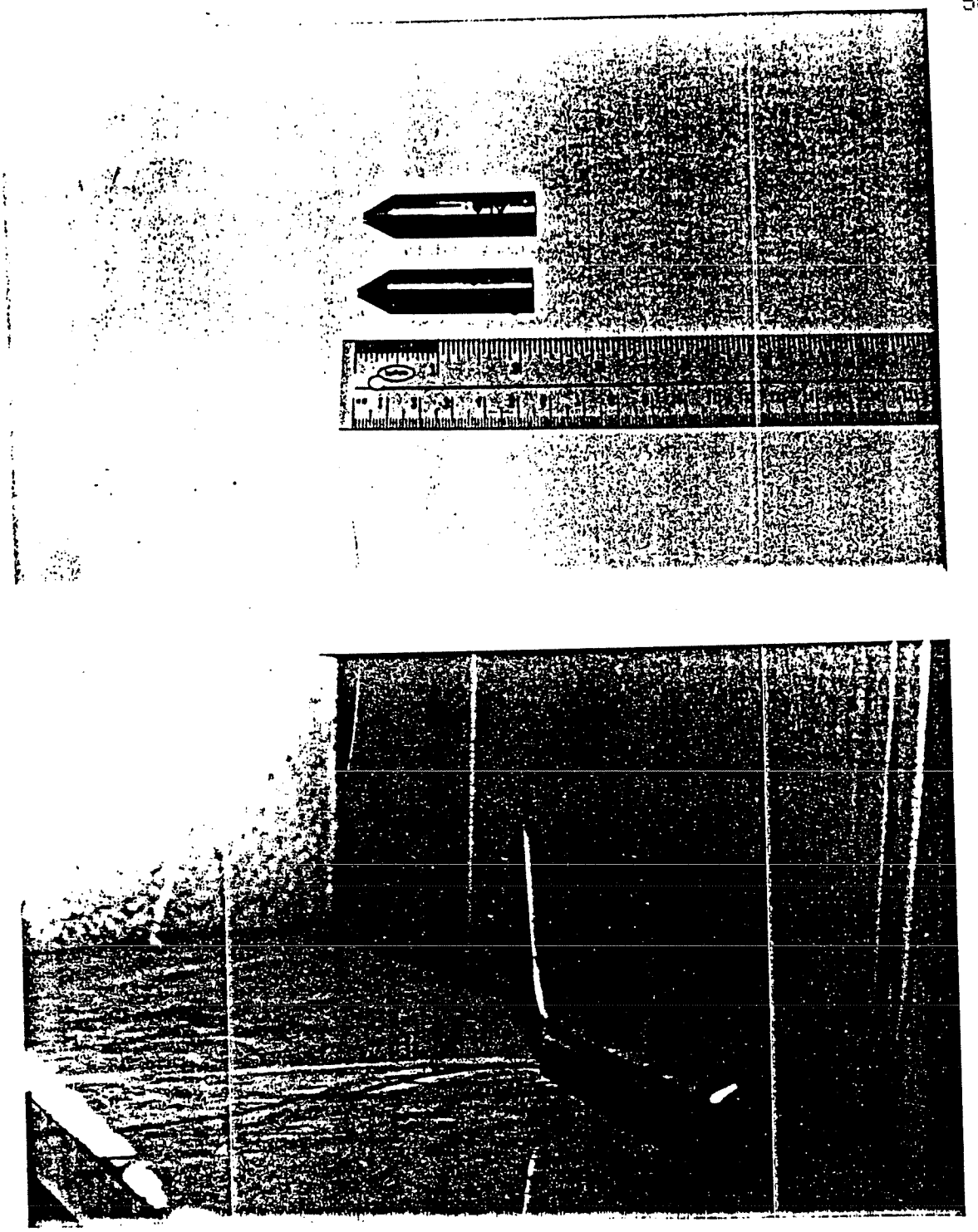

Figure 6.b Device for measurement of liquid phase impact pressure.

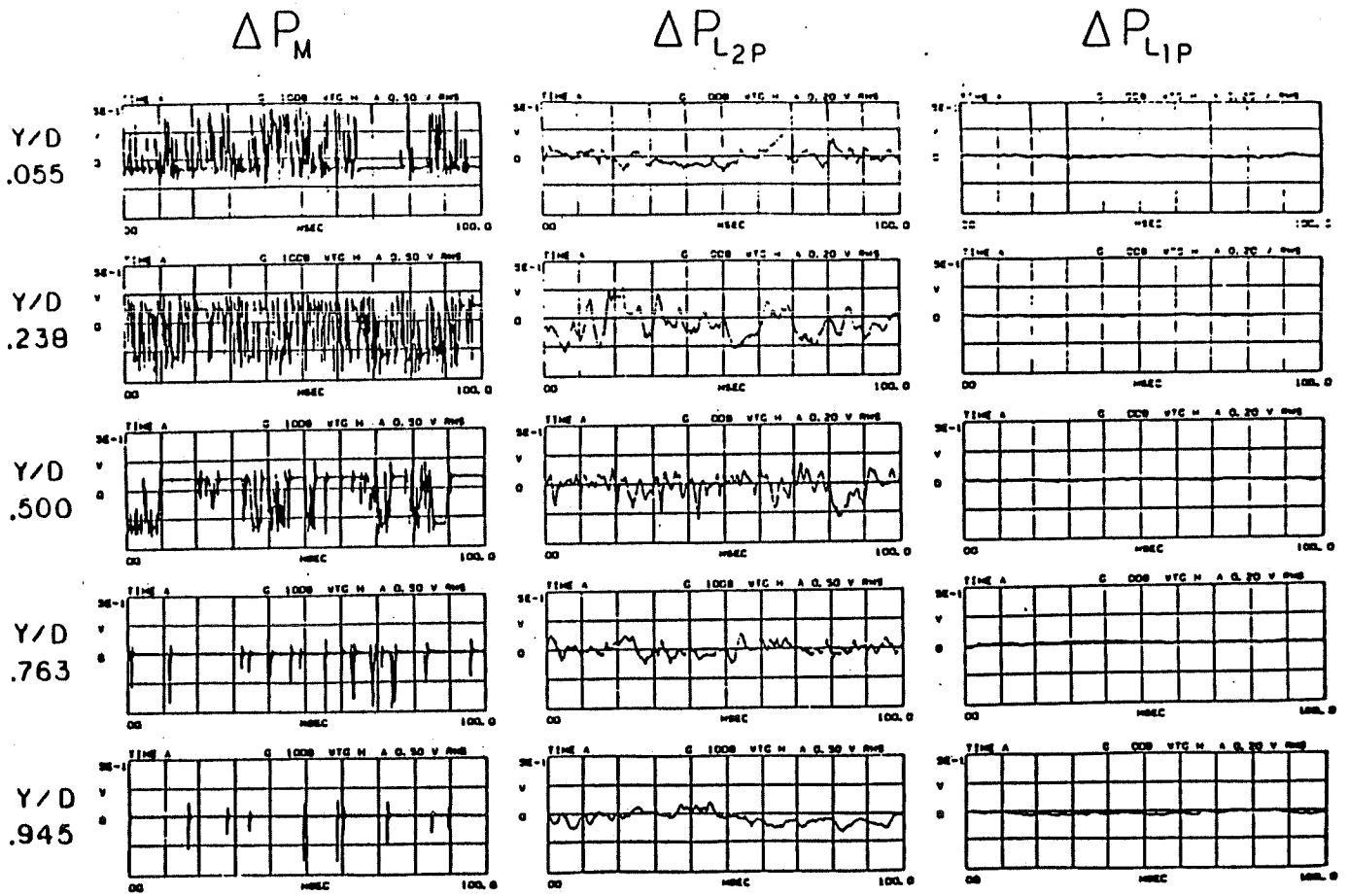

Figure 7.a Typical examples of dynamic pressure signals recorded at axial location 130D and X_o = 0.292.

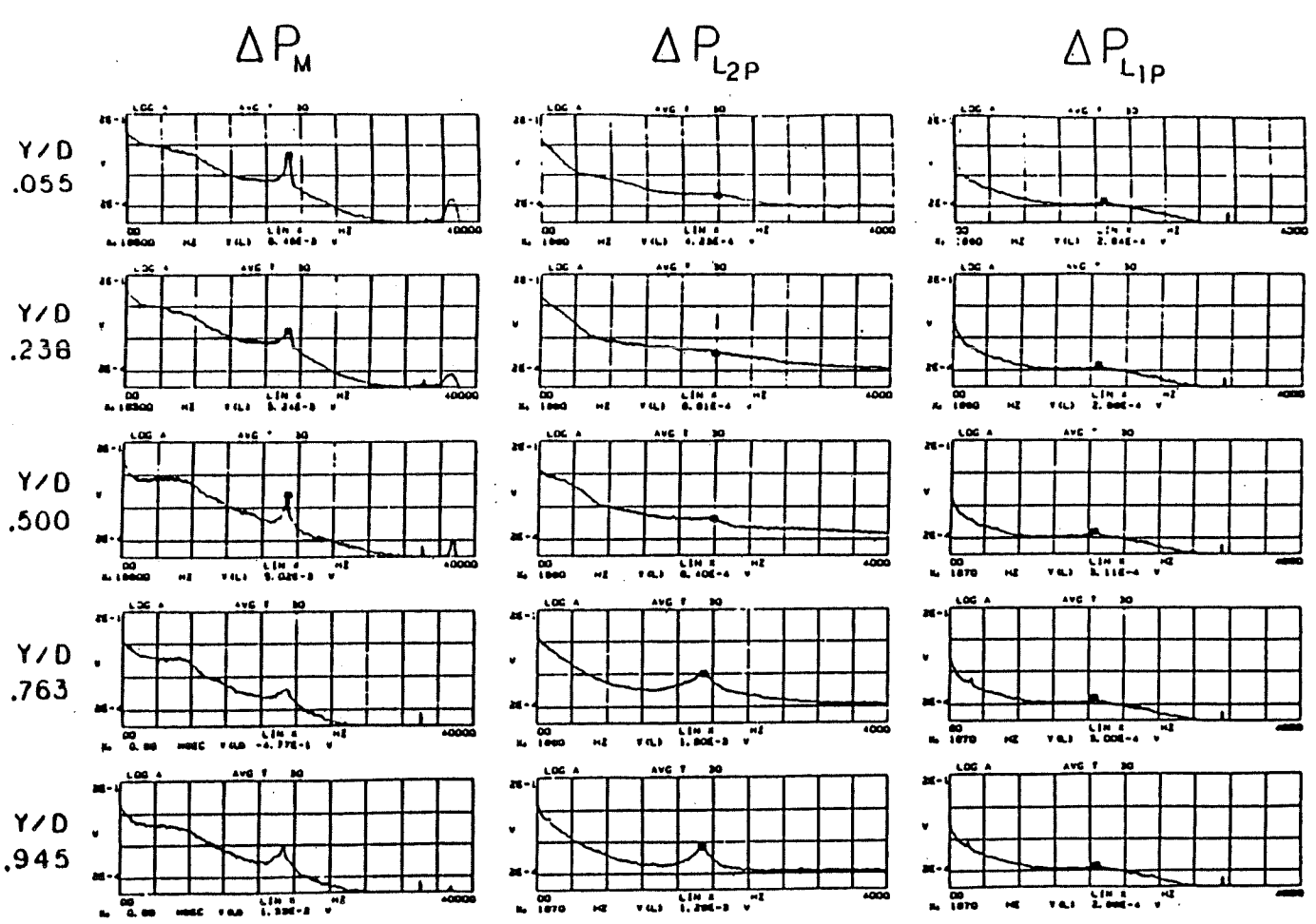

Figure 7.b Broadband frequency spectrum of dynamic pressure signals obtained in Figure 7.a.

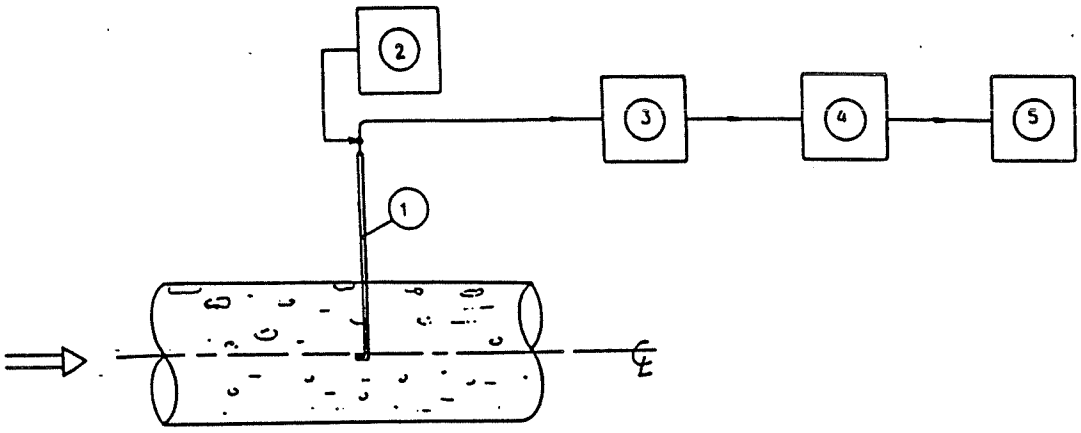

1) Miniature pressure transducer (XCQ-080-50D, with or without isolator)
2) Power suppy (5 V Dc).
3) Amplifiers, Filters (ACCUDAIA).
4) Oscilloscope (TEKTRONIC).
5) Voltmeter (TSI 1076).

Figure 8 Principle and equipment for measurement of the dynamic pressure in two-phase flow.

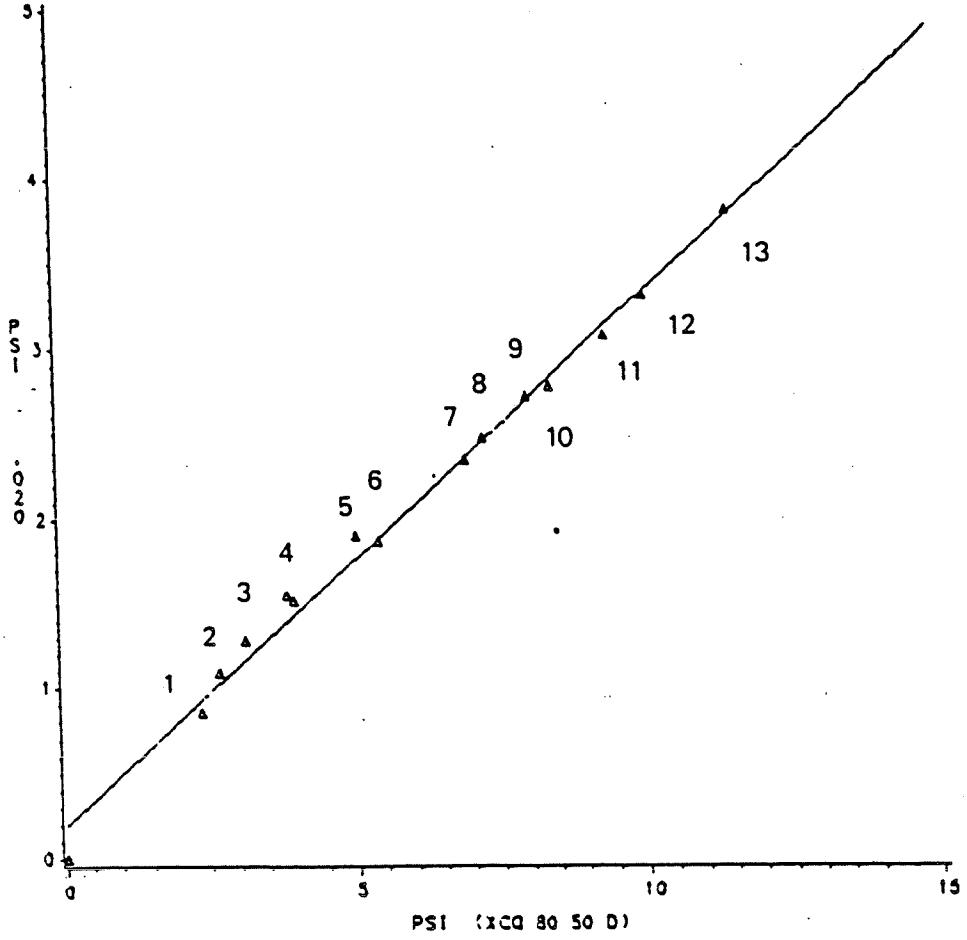

$$(PSI)_{0.020"} = 0.337\ (PSI)_{XCQ-080}$$

USGPM

1-	2100	4-	2750	7-	3580	10-	3945	13-	4750
2-	2240	5-	3080	8-	3660	11-	4140		
3-	2440	6-	3200	9-	3850	12-	4340		

Figure 9 Calibration curve of a liquid phase isolator in water flow (0.020 in. opening width).

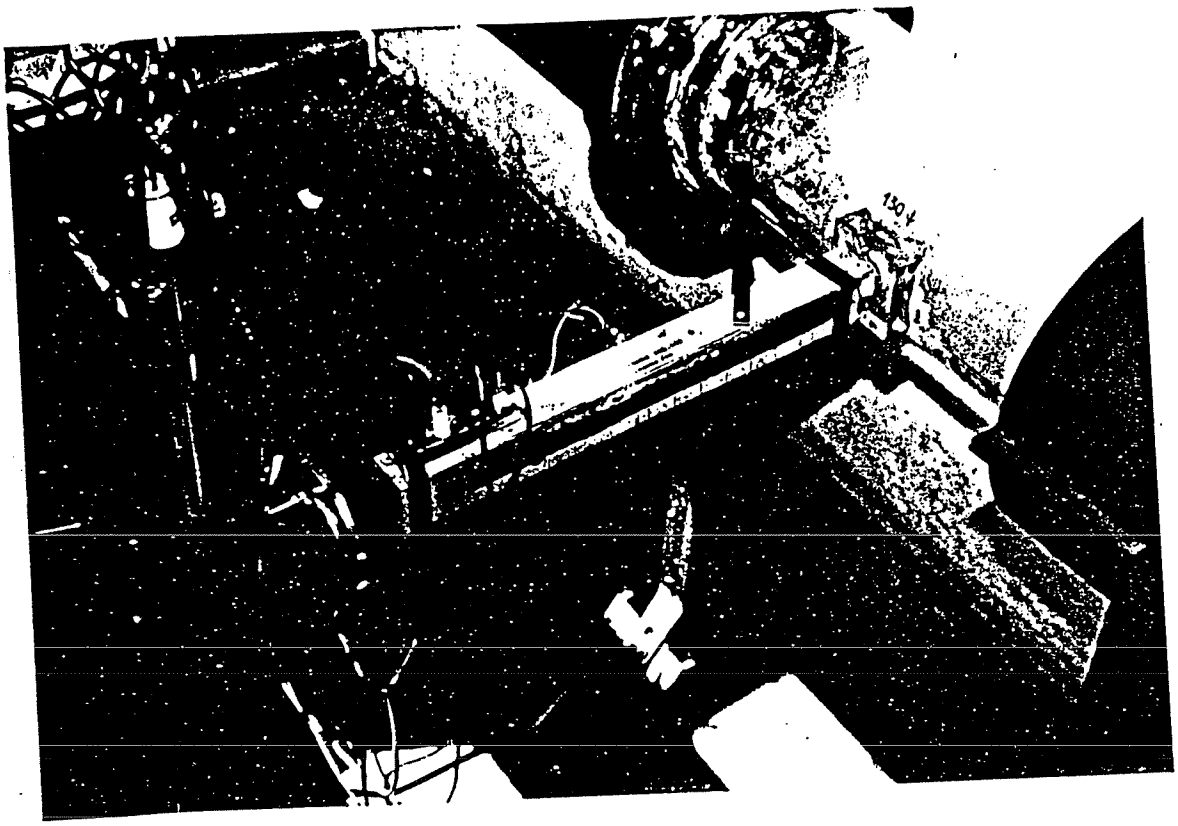

Figure 10 Apparatus used in measurement of impact pressure in cross-sectional planes.

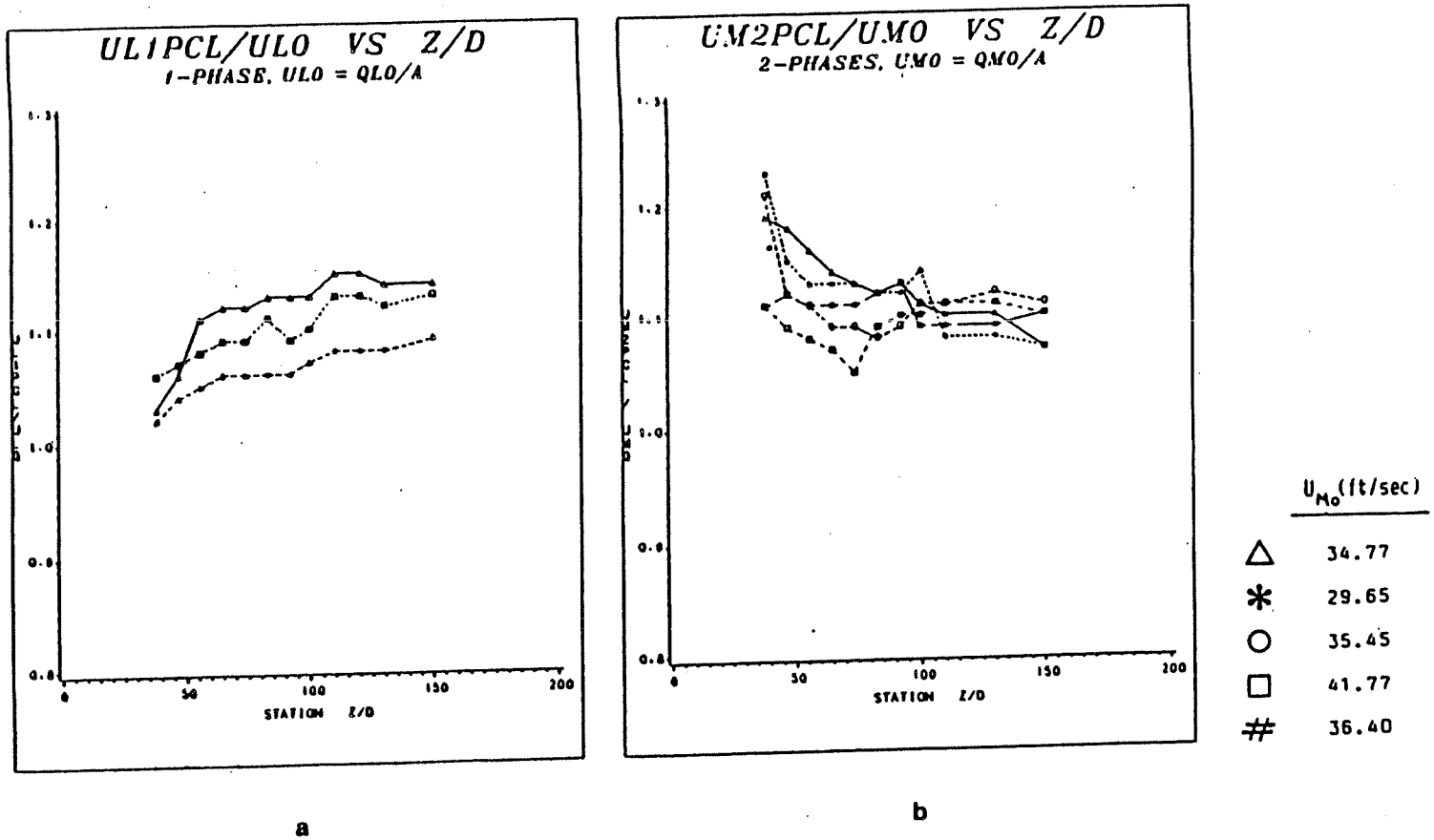

U_{LO} (ft/sec)	
25.77	△
27.69	□
30.74	*

U_{MO} (ft/sec)	
34.77	△
29.65	*
35.45	○
41.77	□
36.40	#

Figure 11 11.a Longitudinal variation of velocity ratios (measured values at pipe axis over superficial values) in two-phase flow.

11.b Longitudinal variation of velocity ratios (measured values at pipe axis over superficial values) in single phase flow.

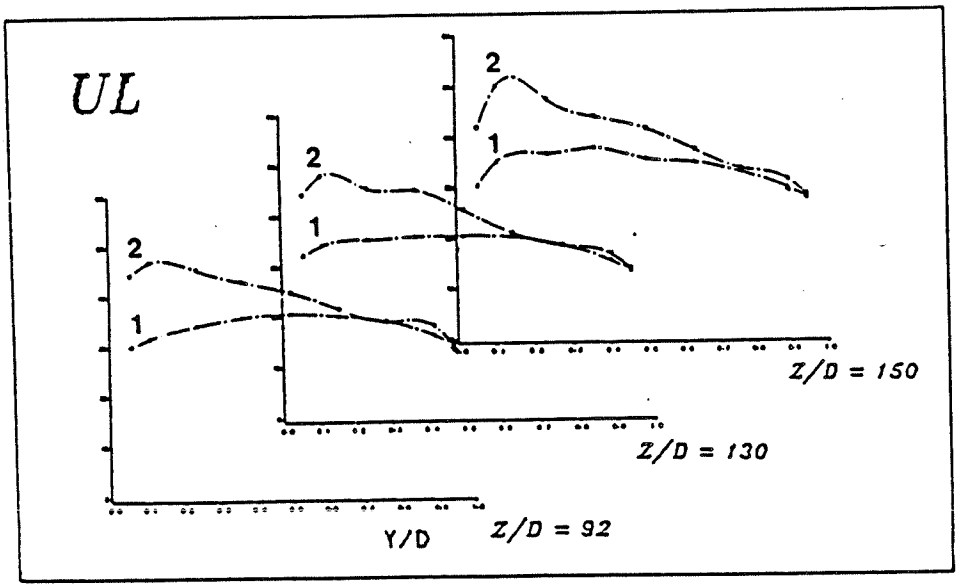

Figure 12 Variation of velocity profiles along 3 axial locations. (1: X_o, 2: X_o = 0.264, Q_{Lo} = 4373 USGPM, U_L ft/sec.).

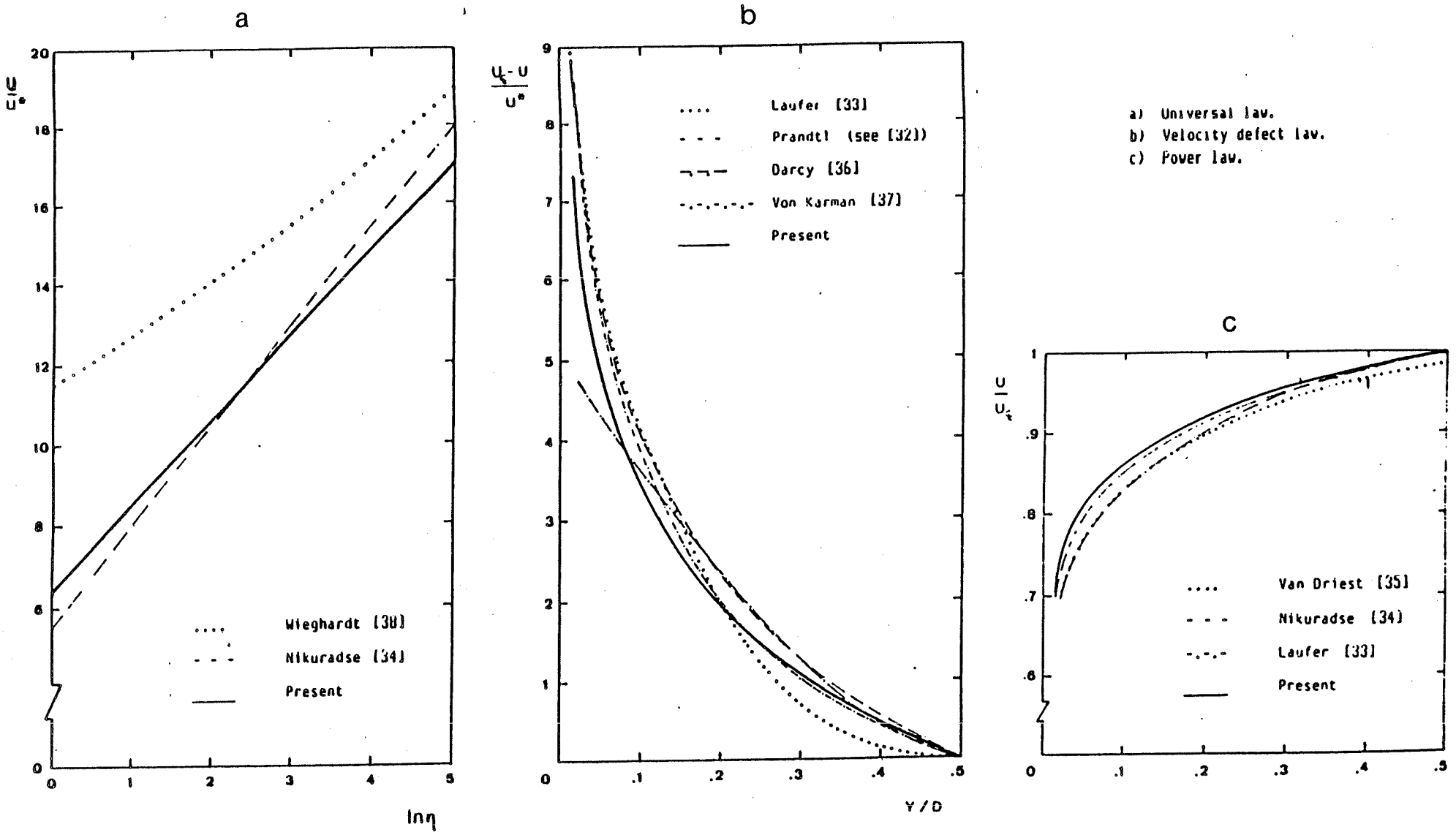

Figure 13 Verification of average velocity distribution laws in single phase flow.

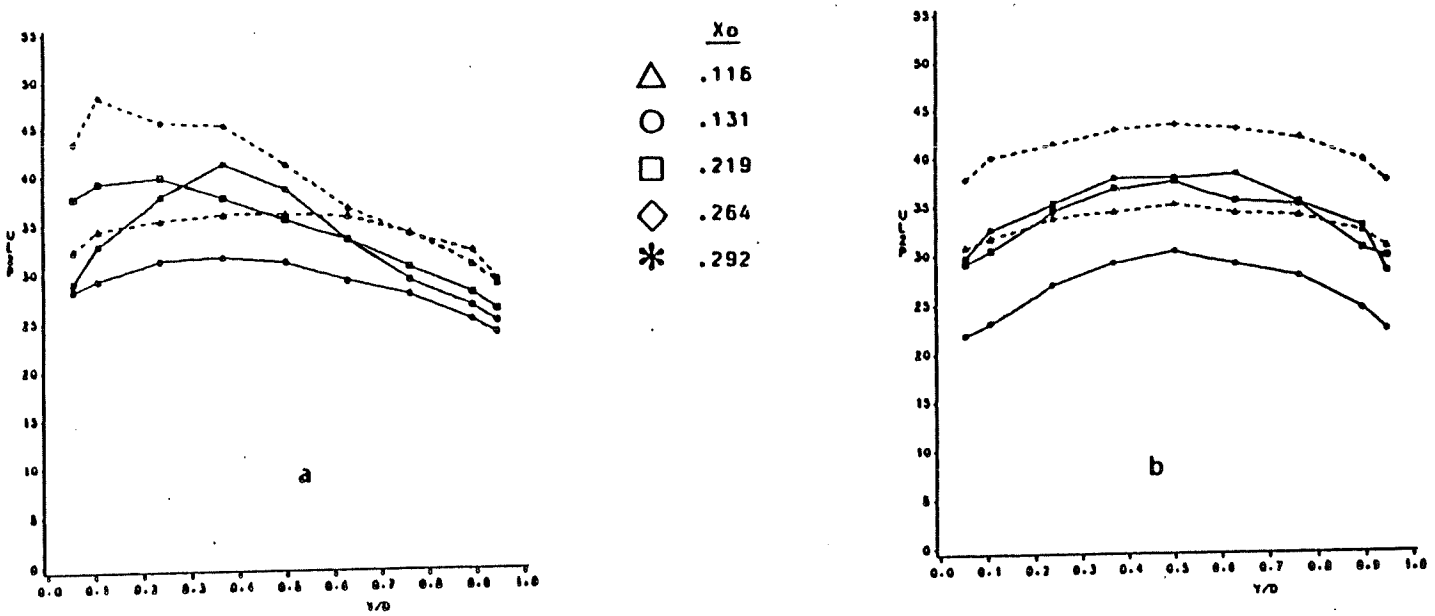

Figure 14 14.a Distribution of liquid phase velocity in transversal plane.
14.b Distribution of liquid phase velocity in radial plane.

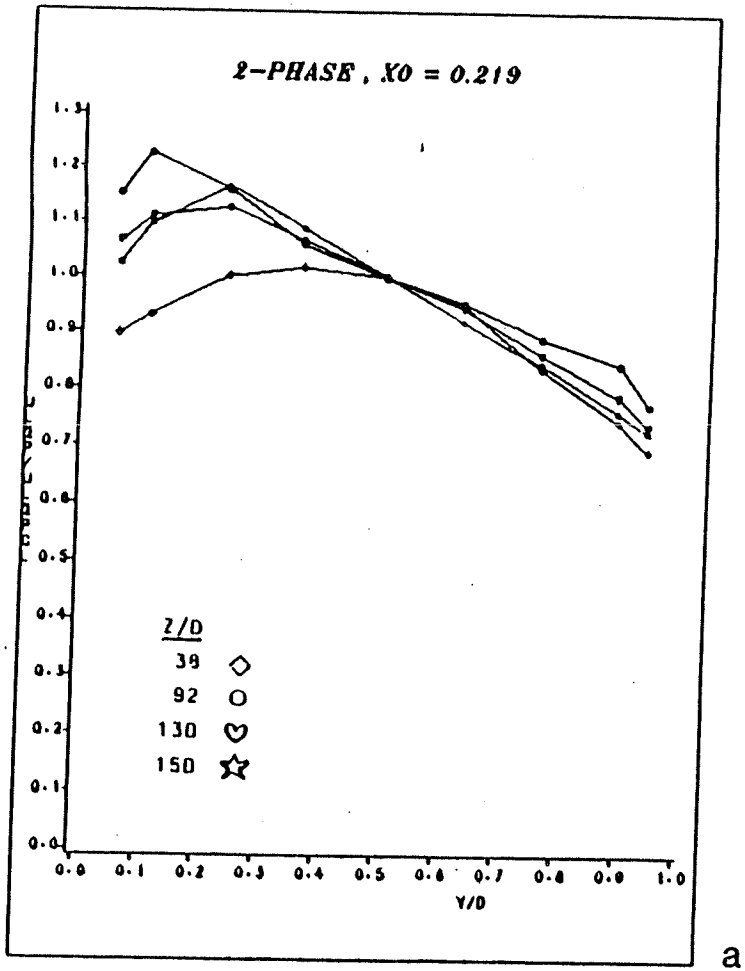

a

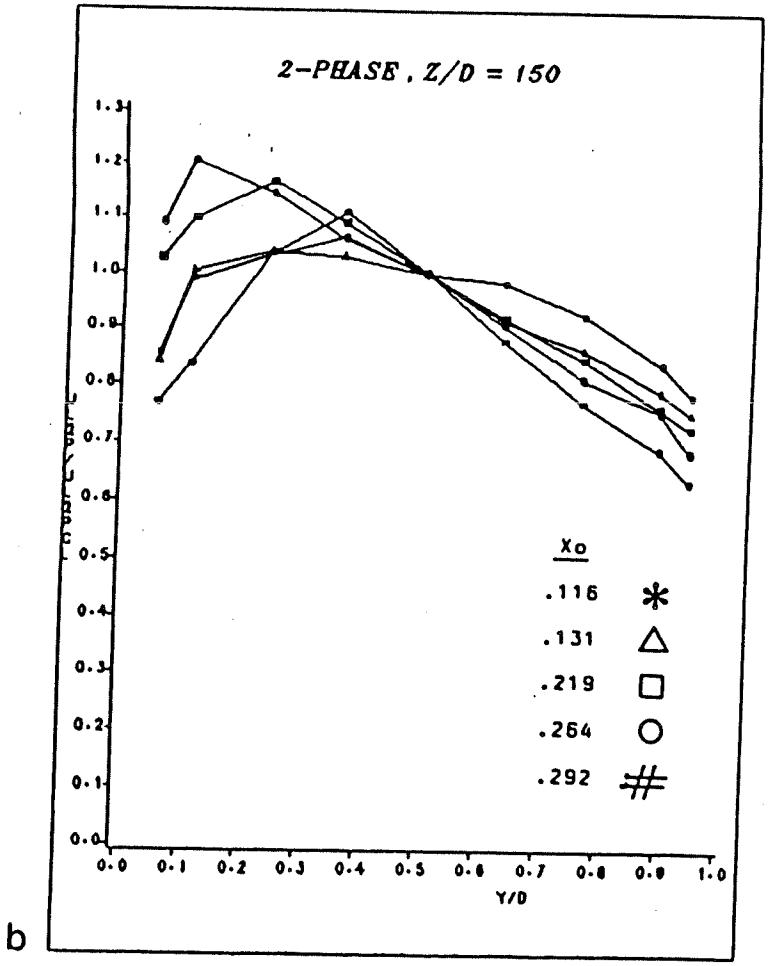

b

Figure 15 15.a Radial distribution of rtio U_L / U_{Lo} at X_o = 0.219 and various axial locations.

15.b Radial distribution of ratio U_L / U_{Lo} at 150 D axial location and various flow folumetric qualities.

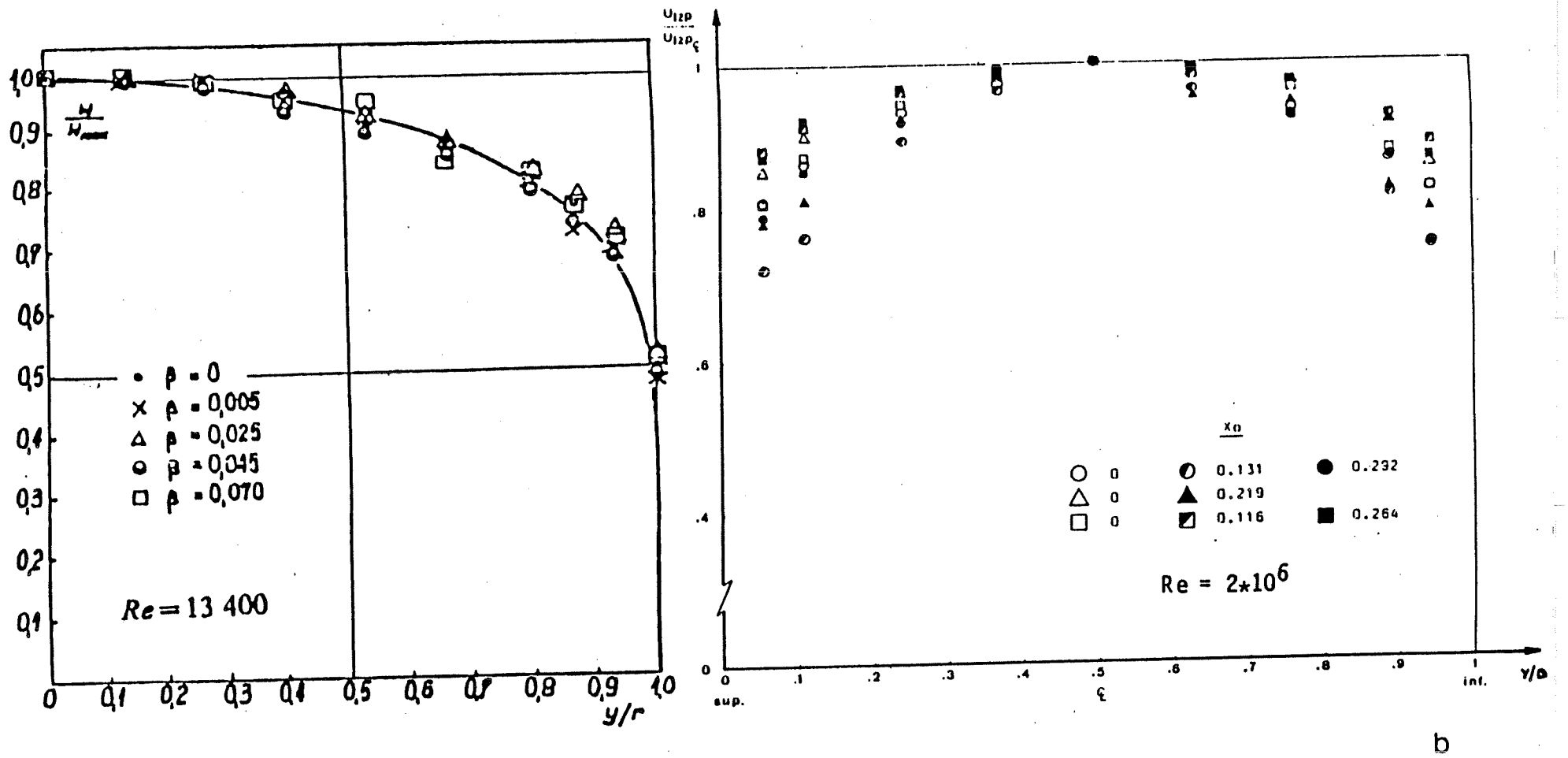

Figure 16 Radial distribution of liquid phase velocity in small diameter pipe [5] and large diameter pipe [present, 8-in.].

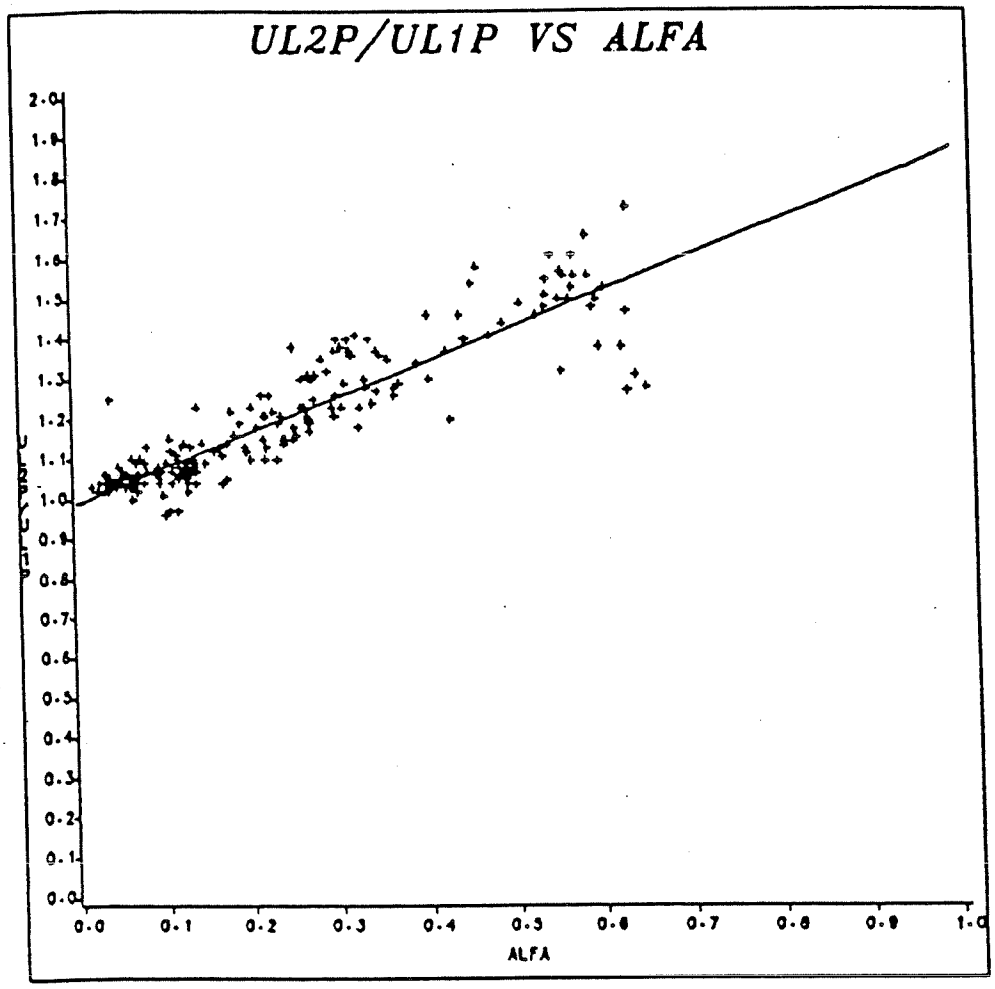

Figure 17 Variation of ratios U_{L2P}/U_{L1P} in terms of void fraction.

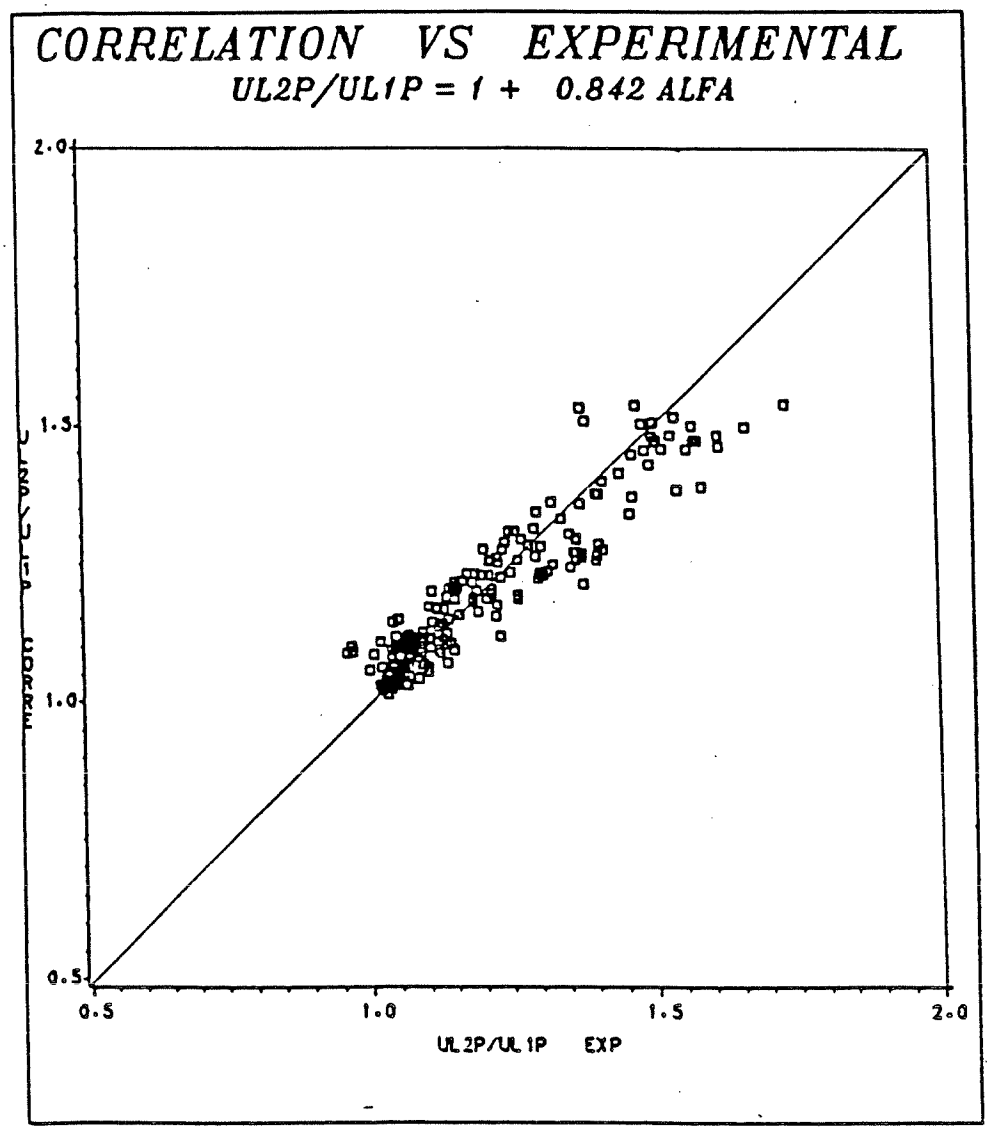

Figure 18 Comparison between values estimated by the proposed correlation and experimental results.

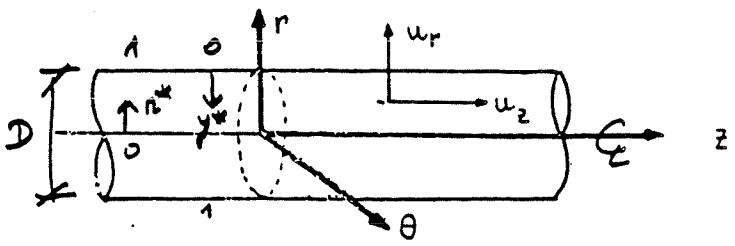

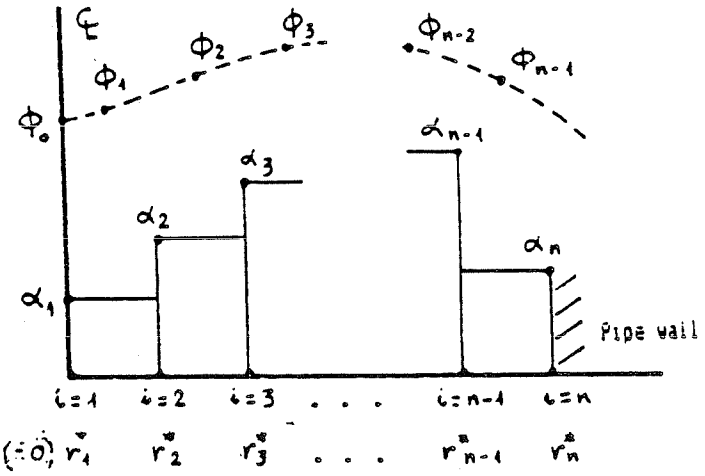

Figure 19 19.a Pipe coordinates.
19.b Steplike arrangement for numerical computation of liquie velocity and void fraction.

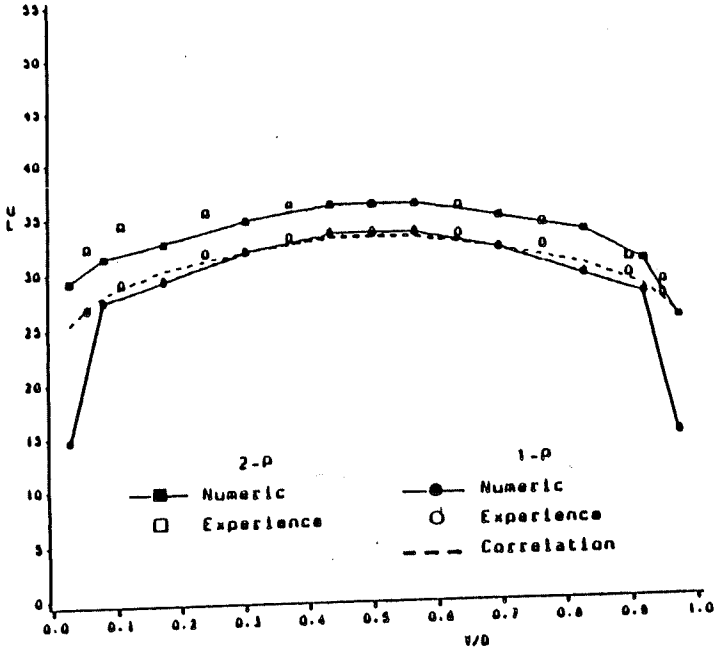

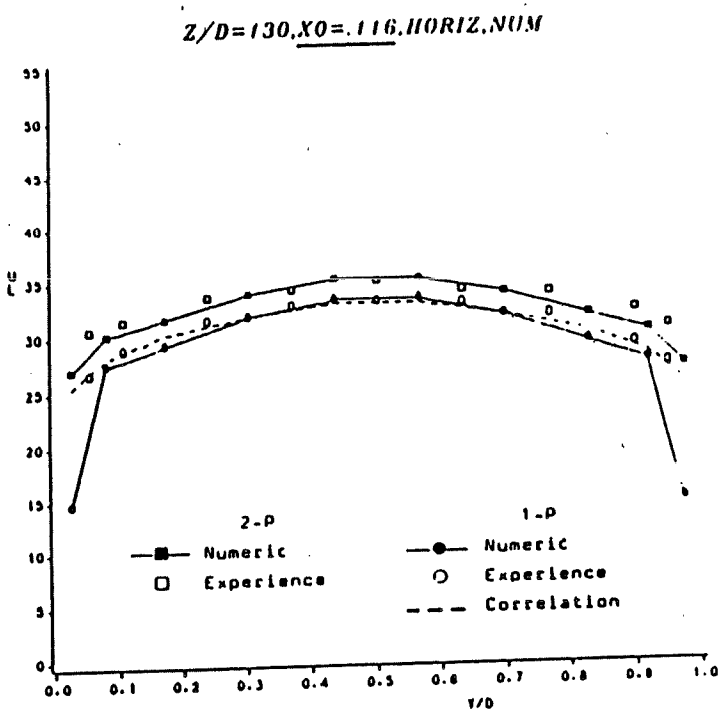

Figure 20 Numerical results of liquid phase velocity profiles (transversal and radial planes).

Z/D=130,XO=.131,TRANS.NUM

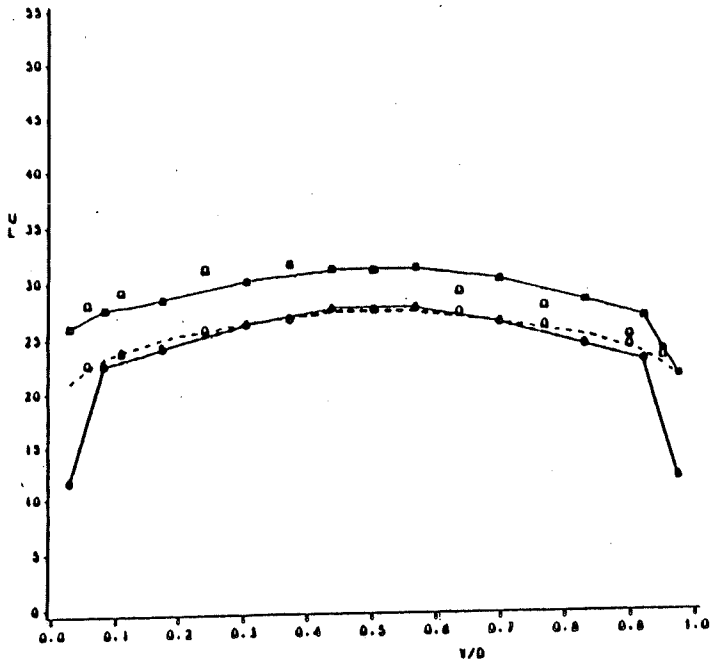

2 - P
Numeric
Experience

Z/D=130,XO=.131,HORIZ.NUM

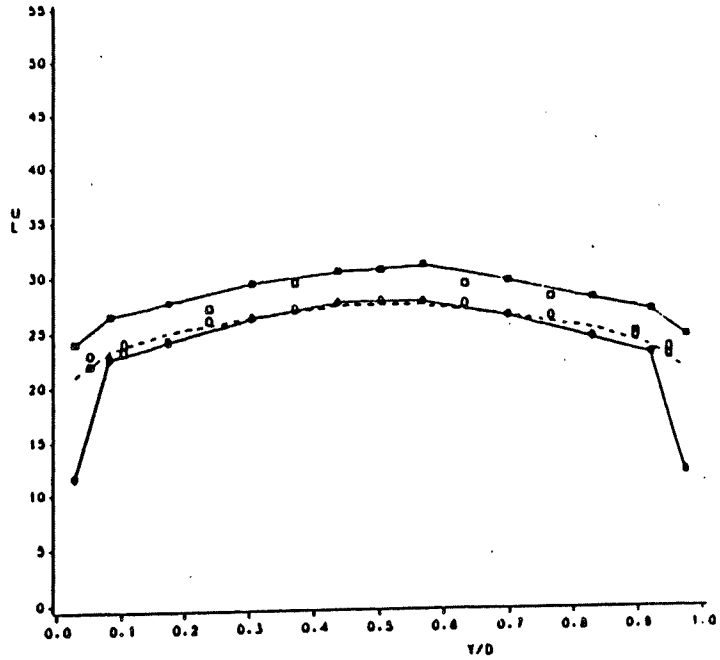

1 - P
Numeric
Experience
Correlation

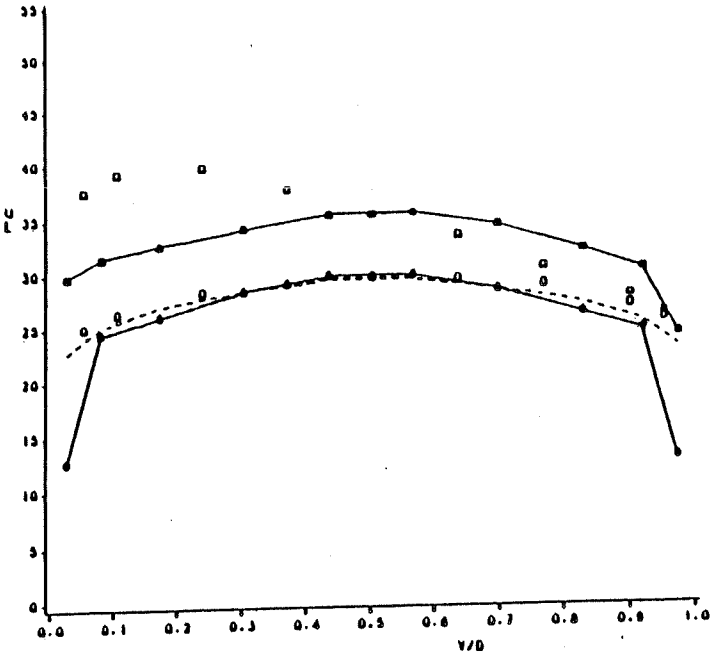

2 - P
—■— Numeric
□ Experience

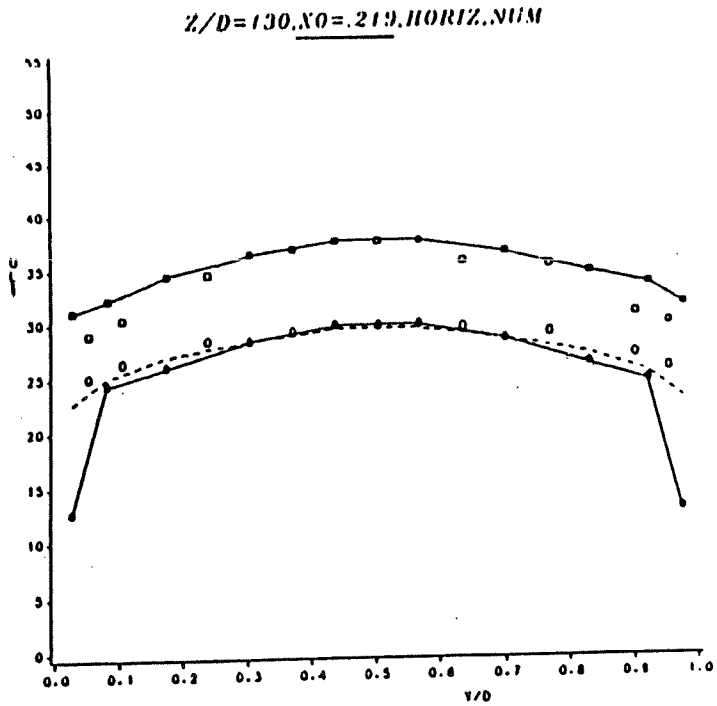

1 - P
—●— Numeric
o Experience
--- Correlation

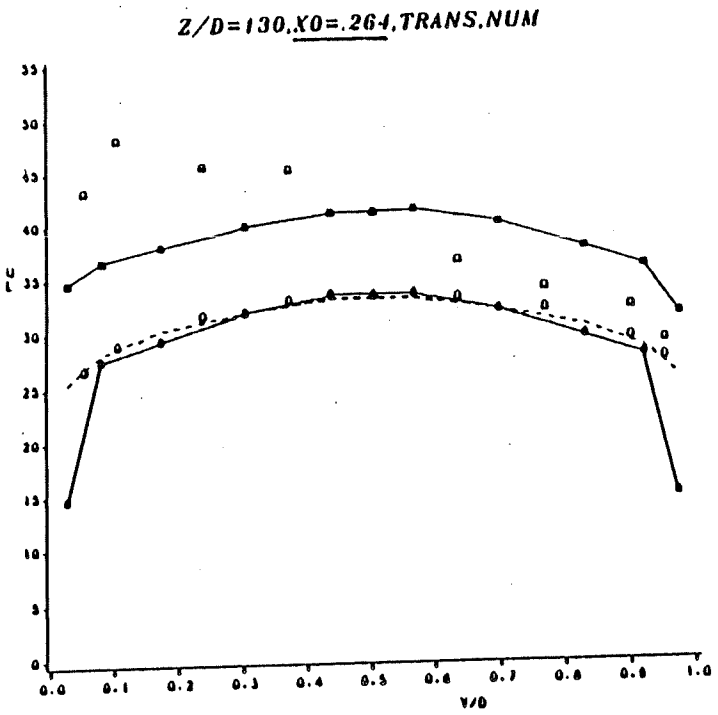
Z/D=1.30,X0=.264,TRANS.NUM
Cp
Y/D
2 - P
Numeric
Experience

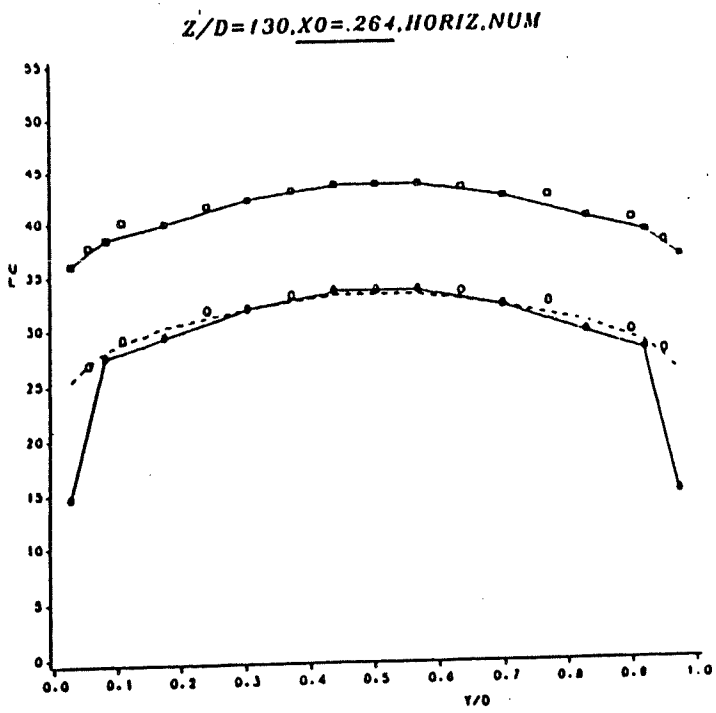
Z/D=1.30,X0=.264,HORIZ.NUM
Cp
Y/D
1 - P
Numeric
Experience
Correlation

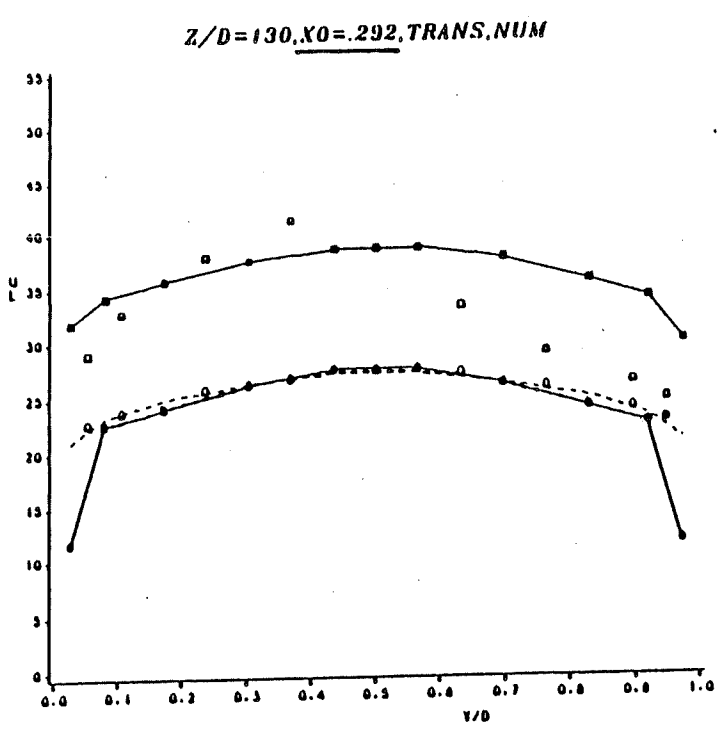

2 - P
Numeric
Experience

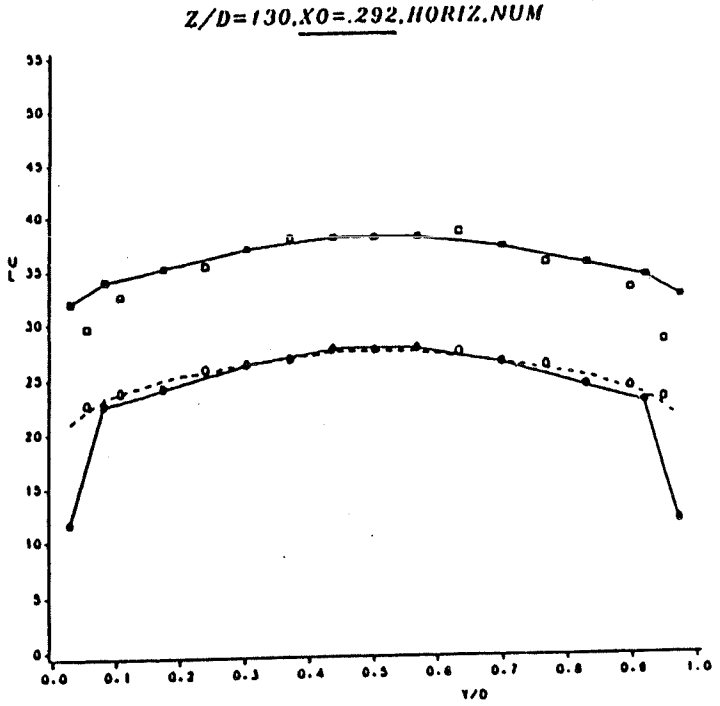

1 - P
Numeric
Experience
Correlation

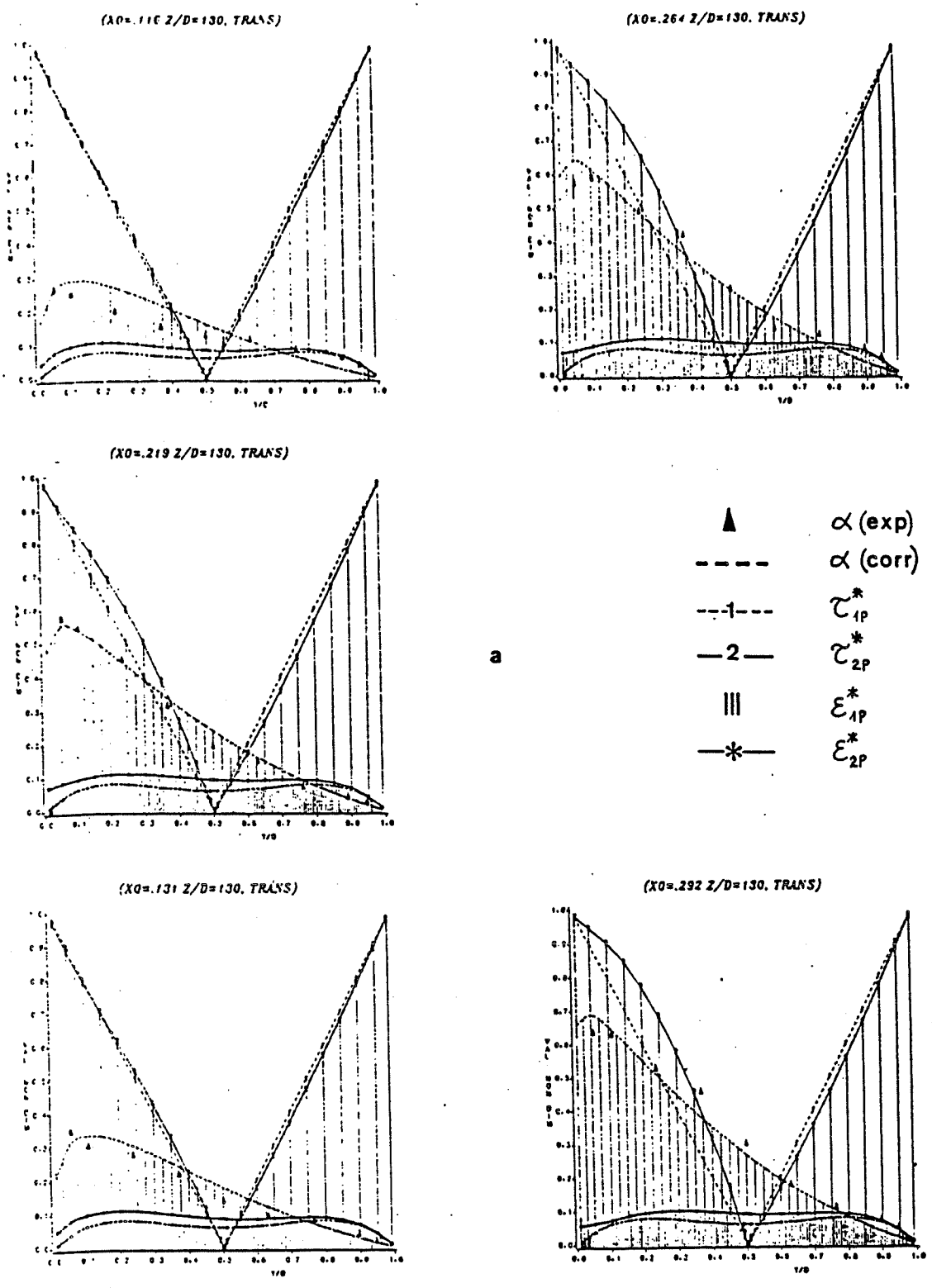

Figure 21 Numerical results of shear stress distribution in dispersed bubbles flow

a) Transversal plane

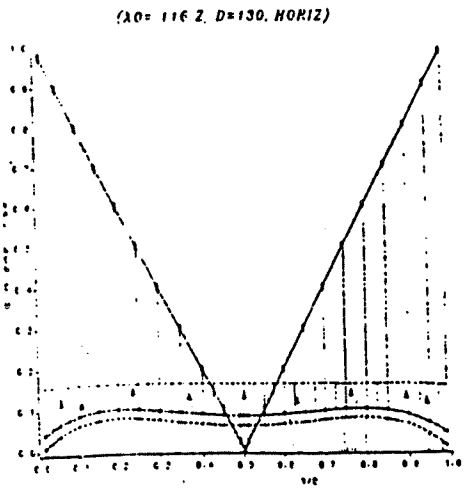

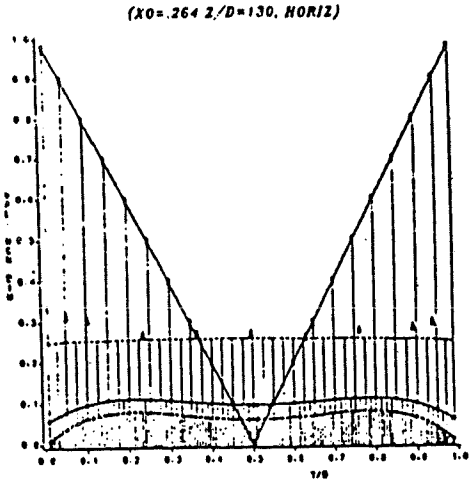

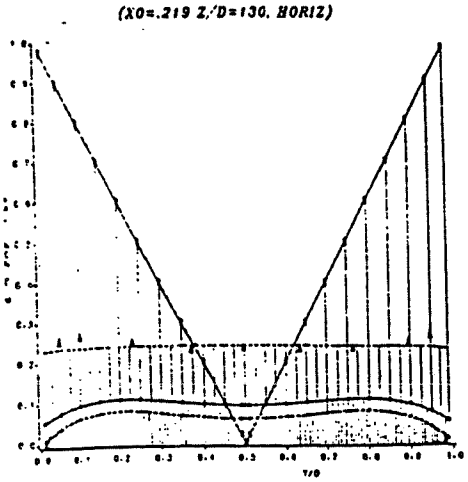

b

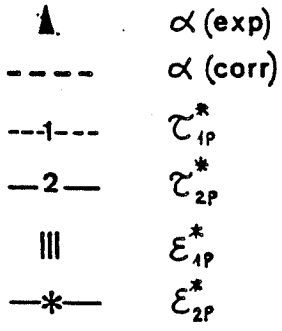

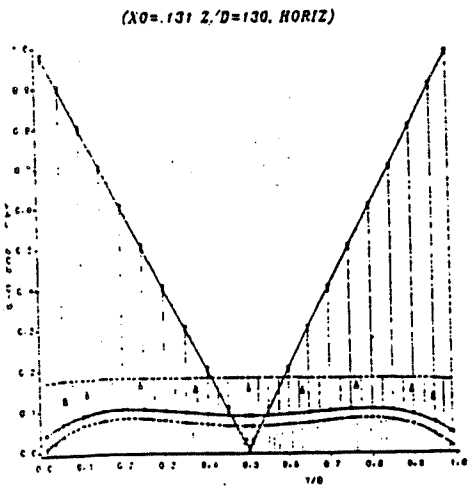

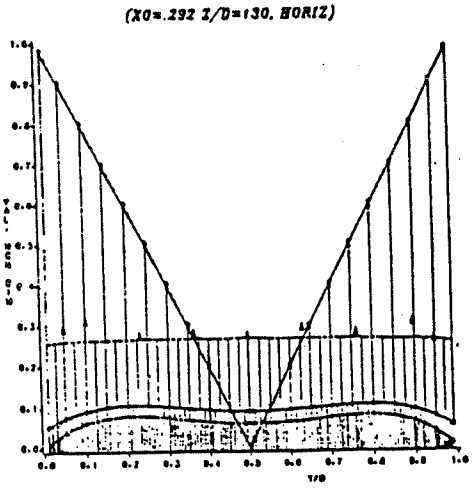

b) Radial plane